Nanotechnology for environmentally sustainable electromobility

Linda Ager-Wick Ellingsen[1]*, Christine Roxanne Hung*[1]*, Guillaume Majeau-Bettez*[1,2]*, Bhawna Singh*[1]*, Zhongwei Chen*[3]*, M. Stanley Whittingham*[4]*, Anders Hammer Strømman*[1]

[1] *Industrial Ecology Programme and Department of Energy and Process Engineering, Norwegian University of Science and Technology (NTNU), Sem Sælands vei 7, NO-7491 Trondheim, Norway*
[2] *CIRAIG, École Polytechnique de Montréal, dép. génie chimique 3333 chemin Queen-Mary, Bureau 310 C.P. 6079 succ. Centre-ville, Montréal, QC, H3C 3A7, Canada*
[3] *Department of Chemical Engineering; Department of Mechanical and Mechatronics Engineering, E6-2006, University of Waterloo, 200 University Avenue West, Waterloo, ON, N2L 3G1, Canada*
[4] *NorthEast Center for Chemical Energy Storage, Binghamton University, 4400 Vestal Parkway East, Binghamton, New York 13902, United States*

This is the peer-reviewed, accepted version of the following article:

Ellingsen, L.A.-W., C.R. Hung, G. Majeau-Bettez, B. Singh, Z. Chen, M.S. Whittingham, and A.H. Strømman. 2016. Nanotechnology for environmentally sustainable electromobility. *Nature Nanotechnology* 11(12): 1039–1051.

Which has been published in final form at:

http://www.nature.com/nnano/journal/v11/n12/full/nnano.2016.237.html

Its digital object identifier (DOI) is 10.1038/nnano.2016.237:

http://dx.doi.org/10.1038/nnano.2016.237

Abstract

Electric vehicles (EVs) powered by lithium ion batteries (LIBs) or proton exchange membrane hydrogen fuel cells (PEMFCs) offer important potential climate change mitigation effects when combined with clean energy sources. The development of novel nanomaterials may bring about the next wave of technical improvements for LIBs and PEMFCs. If the next generation of EVs is to lead to not only reduced emissions during use but also environmentally sustainable production chains, the research on nanomaterials for LIBs and PEMFCs should be guided by a lifecycle perspective. In this Review, we describe an environmental lifecycle screening framework tailored to assess nanomaterials for electromobility. By applying this framework, we offer an early evaluation of the most promising nanomaterials for LIBs and PEMFCs and their potential contributions to the environmental sustainability of EV lifecycles. Potential environmental trade-offs and gaps in nanomaterials research are identified to provide guidance for future nanomaterial developments for electromobility.

1. Introduction

Anthropogenic greenhouse gas emission rates increased by more than 80% from 1970 to 2010[1], and emissions from the transport sector increased at a faster rate than any other energy end-use sector[2]. In 2010, transportation was responsible for 23% of total energy-related CO_2-emissions[2], with total energy consumption reaching 27% of the total end-use energy, of which about half was consumed by light-duty vehicles[2]. There is currently an estimated 1 billion light-duty vehicles worldwide, and as a result of increasing standards of living and economic activity, this number is expected to double by 2035[3], with obvious repercussions for energy security, climate change and urban air quality.

Vehicles with electric powertrains are seen as attractive alternatives to conventional internal combustion engine vehicles[2], and many governments have introduced policies promoting market uptake of electric vehicles (EVs)[4,5]. With the increasing market for EVs, major automobile manufacturers now have one or more EVs in their production line. The remarkable drop in the cost of LIBs over the last decade will accelerate the adoption of EVs[6]. When combined with clean energy sources, EVs can offer a range of advantages over conventional vehicles, such as reduced greenhouse gas emissions and local air pollution[7,8] and improved energy efficiency[9]. However, a shift in drivetrain technology to LIBs and PEMFCs leads to changes in supply chains, introducing more environmentally intensive materials and production processes in exchange for potentially lower operating emissions[10]. Thus, a systems perspective, such as that provided by life cycle assessment (LCA), is required to understand the environmental implications arising from transport electrification. LCA offers a way to quantify environmental impacts associated with the production, use, and waste handling of goods and services[11] (see Box 1).

Due to their unique electrical and mechanical properties only attainable at the nanoscale, active nanostructured materials developed for LIBs and PEMFCs may significantly improve their performance. Nanomaterials can notably offer advantages over bulk-structured materials through reduced diffusion lengths of ions and electrons, and in some cases, through changes in the phase diagram resulting in changes in reaction mechanism. However, the synthesis of nanomaterials may be more energy demanding[12] than that of their bulk counterparts, which in turn can have significant bearings on the lifecycle environmental impact of EVs[13], particularly with respect to greenhouse gas emissions. For EVs to offer environmental benefits, the potential technical improvements introduced by nanomaterials must be greater than environmental impact of EV production.

In this review, we investigate how nanomaterials can contribute to more environmentally sustainable electromobility and compare different candidates for development in this direction. For the purpose of this study, the term EVs includes vehicles with a fully electric drivetrain using lithium ion batteries (LIBs) or proton exchange membrane hydrogen fuel cells (PEMFCs). In section 2, we briefly review the LCA literature of EVs to identify potential trade-offs and sources of environmental impacts of the current state of the EV technology. This serves to identify areas in which the development of novel materials may bring about the greatest improvements from a systems thinking perspective. In Section 3, the challenges identified in Section 2 are grouped into three lifecycle attributes through which nanotechnology may contribute to the development of more environmentally sustainable batteries and fuel cells for electric transport. We then evaluate and compare different nanotechnological developments and challenges with respect to the three lifecycle attributes for batteries (Section 4) and for fuel cells (Section 5). Section 6 distils the overarching evaluations from the previous sections and provides insights into the contribution of nanotechnologies for more environmentally sustainable mobility.

2. Life cycle assessment of electric vehicles

Several academic studies have assessed the environmental impact of EVs[7,10,14–22]. Studies assessing EVs and relevant components have assumed LIBs for battery electric vehicles[22–25] and PEMFCs for fuel cell vehicles[10,15,20,21]. Compared to conventional vehicles, a larger share of EVs' lifecycle impacts occur in the material processing and vehicle production phase, notably because of their reliance on relatively scarce materials and on production processes with high energy requirements[10,14,15,19]. Consequently, studies have found up to 40-90% higher greenhouse gas production-phase emissions for EVs compared to conventional vehicles. Whether or not EVs can compensate for their higher up-front environmental impact depends on the emission intensity of electricity sources and hydrogen for charging LIBs and fuelling PEMFCs, respectively. A lifecycle perspective is therefore required when evaluating their environmental performance[7,10,14,19].

Studies assessing impact categories beyond climate change find that EVs can offer substantial positive improvement during its use phase, such as reductions in photochemical smog and fossil resource depletion[8,19]. However, EVs can also have a negative impact in other categories (e.g., human toxicity, freshwater ecotoxicity, metal depletion), mostly arising from material extraction in the production chain[14,19,20,26].

Because of the relatively high environmental impacts associated with the production of LIBs and PEMFCs, the lifetime expectancy and the recyclability of these energy devices are key parameters in determining their lifecycle environmental performance. Several studies have pointed to challenges with PEMFC durability due to degradation in the membrane and catalyst layer during long-term operation[27–29]. Battery EVs, on the other hand, generally suffer from limited driving ranges, and whilst larger batteries allow for longer driving ranges, they also cause more production-phase impacts and add weight to the vehicle, thereby increasing electricity consumption during EV operation[30].

As many excellent reviews already cover the contribution of nanomaterials to overcoming technological and commercialization challenges of LIBs and PEMFCs[31–36], this review rather screens the environmental effects arising from the use of nanomaterials in these devices. For example, while the battery literature indicates that increasing volumetric energy density is an important factor for LIB adoption in battery EVs due to the limited space available[37–40], the LCA literature rather focuses on the need for higher gravimetric energy density to avoid the additional material production and use-phase energy consumption associated with the transport of heavier batteries[7,18,19,23,25].

3. Lifecycle approach for early environmental screening

LCAs strive to guide product development by quantifying all environmental impacts associated with each product, but such a comprehensive assessment is typically limited by data quality and quantity. Multiple simplified, or streamlined, LCA methods have been proposed as a first iteration toward complete LCAs[41–43] in order to provide lifecycle guidance as early as possible in product design, that is, before the design is decided and improvement options restricted. In contrast to full LCAs, there is no standard method to guide the performance of these scoping approaches. In this article, we develop a framework that draws elements from streamlined LCA methods, the qualitative Environmentally Responsible Product Matrix scoping approach[41–43], and key principles of green chemistry[44,45]. These elements are adapted, combined, and updated to address the parameters that both can be influenced by nanotechnological research and determine environmental impacts of EVs. The development of the framework is made all the more pertinent by the fast pace of nanotechnology research, the great diversity of competing nanomaterials, and their differing technological readiness levels, which ranges from laboratory-scale proof of concept to commercialization.

The framework used here appraises nanomaterial candidates with respect to three lifecycle attributes: e*nvironmental intensity of materials*, *material and weight efficiency*, and *energy efficiency*, which are described in detail below and illustrated in Figure 1. Together, these lifecycle attributes cover all lifecycle phases of the material: production, use and end-of-life. To guide action, we distinguish between intrinsic parameters that are attributed to the material itself, and value chain parameters that are characteristic not of the material but of the activities involved in its production. The evaluation of materials is adapted to the special nature of electromobility. Section 3 in the Supplementary information describes the criteria and basis of comparison and provides further details in Tables S1-S5 and Figures S4-S9.

Environmental intensity of materials

The environmental intensity of a material describes the extent to which producing and using a given mass of a given material causes damages to the lifecycle areas of protection: human health, ecosystems, and resource availability (Box 1). For example, energy intensive extraction or production processes can result in high greenhouse gas emissions, which in turn can lead to damages to human health and ecosystems. This lifecycle attribute is highly relevant since, on the one hand, LCA studies on EVs find that materials used in LIBs and PEMFCs have environmentally intensive extraction and refining processes[10,14,15,19], and since, on the other hand, nanotechnological developments are likely to alter the materials used in LIB and PEMFC productions. Some materials can themselves cause damages through *exposure risks and hazards*. The use of non-renewable materials can increase resource *scarcity,* while material extraction and processing activities throughout the production chain result in embodied *damage to human health* and *damage to ecosystems.* Reducing the particle size from bulk material to a nanoscale can change both the material properties (e.g., increased reactivity) and lead to differing environmental intensity (e.g., *damage to human health*).

Material and weight efficiency

The material efficiency characteristic is a metric of the functionality that a material can achieve per unit of mass. As the environmental aspects of materials as described in the previous section scale directly with the amount of material used, we should strive to attain the same functionality with less material. Given the relatively high environmental impacts associated with material processing in the production of LIBs[22,24,46] or PEMFCs[10,15,21] for EVs, optimizing the utilization of the materials in these devices is important. Increasing gravimetric *energy density* in LIBs or *power density* increases the material efficiency as less material can be used for the same energetic output. Improvements in material *lifetime and stability* allow for devices that last longer and in turn can reduce the need for replacement, thereby avoiding the use of additional materials. *Energy density, power density,* and *lifetime and stability* of nanomaterials were compared to the performance of commercial 'baseline' material. Reducing *material losses* during synthesis and increasing the *recyclability* both improve material efficiency by minimizing waste. The use of nanomaterials in LIBs and PEMFCs may affect the material efficiency (e.g., change in energy or power density) due to large surface areas, but it may also result in unwanted side-reactions (e.g., influence lifetime and stability). Material efficiency considerations such as energy and power density allow for lighter batteries and PEMFCs; these lightweighting effects also provide side benefits in the form of gains in energy efficiency.

Energy efficiency

Energy efficiency is a measure of how much functionality a given energy input can provide; here we consider energy losses during operation and energy use in the synthesis of nanomaterials. Depending on the energy sources used for producing electricity or hydrogen, the energy losses in LIBs and PEMFCs during operation can contribute to a substantial share of the device's lifecycle greenhouse gas emissions and other environmental impacts[9,19,24,25]. Here, we consider the *device efficiency* to measure how well nanomaterials enable the device to transform and deliver energy. LCA studies find that energy consumption in the value chains of LIBs can also contribute significantly to their greenhouse gas emissions and production impact[24,25,46]. *Energy of nanosynthesis* measures how energy efficient the manufacturing processes of nano-enabled LIB and PEMFC materials are. While using nanomaterials instead of bulk materials may improve the device efficiency due to increased reactivity, the differing methods to synthesize these nanomaterials require varying amounts of energy. As energy is often produced from carbon intensive sources, energy use often translates to greenhouse gas emissions.

In the following sections, qualitative and semi-quantitative comparisons will be performed in terms of the three lifecycle attributes for various nanomaterials. Figures 2-5 use colour coding to illustrate the perceived relative strengths of different nanostructure materials with respect to the above lifecycle attributes. Green denotes relative strength, red relative weakness, yellow intermediate characteristics, and white a lack of data. Nanostructures are given by circles, whereas the paler background indicates the characteristics of the material in bulk form. Absence of a circle indicates a lack of data relevant to nanostructures. The grey background denotes the 'baseline' material. Although many of these lifecycle attributes pertain to the device as a whole (e.g., energy density, power density, and lifetime), we will consider the materials in isolation for greater ease of analysis. Thus, a cathode with high specific capacity and operating voltage will be described as a "high energy density cathode"[38] because its combination with an appropriate anode allows for a high energy density LIB.

4. Nanotechnologies in battery developments

Battery cells are composed of several key components: anode, cathode, separator, electrolyte, and current collectors. However, their energy density and environmental footprint are mainly determined by the properties of the electrode materials[39]. We therefore focus on the environmental performance of different nanostructured anode and cathode materials.

Anode materials

The use of pure lithium anodes is precluded in rechargeable LIBs with liquid electrolytes because of the formation of lithium dendrites on charging, which short the cell, leading to thermal runaway and fires[36]. Due to this increased reactivity and the associated safety issues, pure lithium anodes in nanoform are, so far, unsuitable for LIBs. Most current LIBs rely on the intercalation of lithium ions in anodes predominantly composed of graphite[47–49]. More recently, the use of nanosized lithium titanium oxide spinel ($Li_4Ti_5O_{12}$, LTO) has also been adopted. In addition to these commercial anode materials, multiple alloys and conversion anode materials are currently under research. Figure 2 presents the material lifecycle attributes of reviewed anode nanomaterials, as well as graphite.

Graphite is an abundant material[47], and its extraction or synthesis has relatively low environmental impact[50,51]. Today, it also requires little energy during its production[22] and allows for batteries with good cyclability[47] and high energy efficiency[52,53]. The main weaknesses of this chemistry from a sustainability standpoint relates to its low material efficiency; its limited energy density leads to heavier, larger batteries[54].

Alternative carbon nanostructures with higher theoretical energy densities are under investigation[34], but neither carbon nanotubes nor graphene have been found to be technically feasible because they have too many side-reactions[55]. Carbon nanotubes and graphene also exhibit more environmentally intensive[50,51] profiles and, like other carbon nanostructures, their handling requires more precaution[56] than graphite[57]. The current carbon nanotube synthesis routes are energy intensive[58–60]. Even when potential economies of scale are taken into account, energy requirements for the synthesis of carbon nanotubes through chemical vapour deposition, arc discharge, or laser-assisted methods all remain significant[61], which in turn result in high greenhouse gas emissions[62]. Further, carbon nanotubes anodes have lower charge-discharge energy efficiencies[34,52]. Increasing evidence points to toxicity effects of carbon nanotubes similar to those of asbestos fibres[63,64], which may affect production and end-of-life processing and recycling of the batteries[65].

LTO is obtained from relatively abundant resources[47,66] and has moderate production impacts[50,51]. It intercalates lithium in a safer manner than carbon because it is 1.5 volts away from lithium metal deposition[33], but must be nanostructured in order to reach acceptable power densities because of its low conductivity[34]. Contrary to carbon nanotubes, LTO can be synthesized with moderate amounts of energy and low reagent losses, especially if a hydrothermal synthesis route is selected[13,67]. The resulting nanostructured anodic material offers high cycling energy efficiency[47,68], extreme safety[34,] high power density[69], and extended lifetimes[52]. Although LTO is already used in small commercially available EVs[70], the 1.5V operating potential of LTO leads to inherently low energy densities[33], which reduces its material and weight efficiency and thus its environmental desirability for EVs. LTO nanoparticles also pose a high exposure risk[71]. The positive properties of LTO, however, potentially make it an environmentally sustainable candidate for static and high power applications.

Even more abundant than carbon[47], silicon presents the highest theoretical capacity to store lithium of all studied anode materials[52], potentially allowing for high energy density anodes. Refining silicon to metallurgical grade for use in the chemical industry causes moderate damages to human health and ecosystems[50,51]. Regarding electrochemical performances, bulk silicon anodes suffer from poor power density[72] and extreme volume changes (up to 320%[73]) that lead to rapid structural degradation of the electrode[33], resulting in poor lifetime. The material must therefore be nanostructured to ensure that voids can buffer such swelling[34,74]. Silicon nanoparticles in carbon-based nanocomposites and silicon nanowires have shown to improve electrochemical performance and lifetime with cycle life of 1000-2000 cycles[73,75]. Nanostructured silicon anodes thus open the possibility for high material efficiency in the LIB lifecycle, particularly with respect to lifetime[76] and energy and power density[7773]. However, handling silicon nanoparticles in carbon nanostructures[56,78] and silicon nanowires[79] requires some precaution. The most popular technique used to grow silicon nanowires is chemical vapour deposition[75], which has moderate to high energy requirements[60,75]. As a result, the synthesis of nanostructured silicon may result in high greenhouse gas emissions[72]. Furthermore, during the use-phase, silicon anodes also suffer from higher voltage hysteresis[47] and thereby lower cycling energy efficiencies than graphite or LTO.

Tin and germanium can also reversibly alloy lithium. Nanostructured tin-based anodes cycle with a higher Coulombic efficiency than silicon[47], and germanium-based anodes allow for exceptional power densities[34]. However, given the greater scarcity[47,66] of these metals and the environmental impacts of their extraction and refining[50,51], their lifecycle environmental sustainability performance remains unremarkable[57,80,81]. Tin may nonetheless prove attractive because of its superior performance when combined with other elements, such as abundant and low-impact iron (e.g., Sn_2Fe nanoparticles)[82–84].

Many nanostructured transition metal oxides can enter in a conversion reaction with lithium, which in principle offers more options as potential anode materials. Among these, iron oxides such as haematite (α-Fe_2O_3) and magnetite (Fe_3O_4)[34] are by far the most abundant[47,66] and the least environmentally intensive[50,51,85,86], in contrast to more scarce elements[47,66] such as chromium, molybdenum, ruthenium, and cobalt[87–89]. Green synthesis routes for iron oxide nanoparticles should lead to relatively lean use of reagents and energy[54,90]. Though high specific capacities have been demonstrated[54,90], their relatively high voltages during de-lithiation[34] substantially reduces the overall cell voltage and consequently, energy and power density. High voltage hysteresis[68,91] makes all these issues worse and also leads to low cycling energy efficiencies, typically less than 60%. Such low energy efficiencies constitute a major handicap for an otherwise environmentally attractive material.

Cathode materials

The energy density of LIBs is largely determined by the cathode as its practically achievable energy is much inferior to that of the anode[92,93]. There are two broad categories of cathode materials: intercalation and conversion. Intercalation materials are the most widely investigated and are already used as bulk materials in commercial LIBs[47]. Of the conversion-type cathode materials, none have reached commercialization[47,94]. Figure 3 presents the material lifecycle attributes of reviewed cathode nanomaterials. $LiNi_{0.8}Co_{0.15}Al_{0.05}O_2$ (NCA) is considered to be the 'baseline' cathode material.

By far the most commonly used cathodes today are the layered oxides, such as $LiCoO_2$ (LCO). Due to the use of the relatively scarce cobalt[47,66], commercially available LCO causes moderate direct exposure risks[86,95] and embodied damages to human health and ecosystems[50,51]. In addition, cobalt's high cost has led a drive to replace most of it in many applications[96], resulting in the adoption of materials with lower cobalt content such as $LiNi_{1/3}Mn_{1/3}Co_{1/3}O_2$ (NMC) and NCA. The popular NMC and NCA pose exposure risks and hazards because they, as with many nickel-containing compounds, are suspected of being human carcinogens[57,97–99]. Their high energy- and power densities have nevertheless made them attractive as bulk materials, and these materials are already used in EVs[47]. As nanostructures, however, the decomposition of the electrolyte and formation of surface films result in insufficient lifetime for EV applications. Even though these layered oxides are not used in nanoform, alternative materials must have equal or superior energy density while demonstrating better lifetime and stability than bulk NMC and NCA in order to displace them from the EV market.

A promising layered oxide is the lithium/manganese-rich material (LMR) [100], often written as $Li_2MnO_3{\cdot}nLiMO_2$ (where M = Mn, Co, Ni, etc.). LMR contains more than one lithium atom per transition metal and has more manganese than other metals. Here, we focus on $0.5Li_2MnO_3{\cdot}0.5LiNi_{1/3}Co_{1/3}Mn_{1/3}O_2$. Due to its higher content of manganese relative to NMC, LMR is slightly less environmentally intensive than NMC[50,51,98,101]. Furthermore, LMR also has a high voltage and specific capacity that allows for a significant increase in energy density over current commercially available cathode materials[102]. Despite these advantages, poor rate capability[103] result in low power density, whereas thermal safety issues[37] and voltage fade[104] result in poor lifetime and stability, all of which complicate its commercial introduction for EVs.

Lithium iron phosphate (LFP) is found in nature as the mineral triphylite[105] and has low exposure risks or hazards[86]. Furthermore, environmental impacts associated with its production value chain are lower than most other cathode materials[16,50,51]. As a bulk material, LFP has moderate electric potential[47], outstanding thermal stability[52], and excellent cycling performance[106], but its two-phase reaction mechanism, with low ion diffusion rate and very low electronic conductivity[107], makes it difficult to reach capacities close to the theoretical limit[52]. However, research found that in nanoparticle form, the material could produce stable cycling much closer to its theoretical capacity because the phase diagram is changed and the reaction proceeds via a metastable single-phase mechanism[37]. This development increased the material's energy-[52] and power[33] densities, but its energy density remained inferior to that of other commercially available cathode materials such as NMC[47,48]. The lower energy density[47] and the claimed lower charge-discharge energy efficiency of LFP[106] can result in higher electricity use per kilometre driven compared to other cathode materials, which in turn would lead to higher indirect greenhouse gas emissions in the use phase. LFP can be produced through several nanosynthesis methods[108], which particularly influences the energy use, and consequently greenhouse gas emissions, associated with its production. The superior electrochemical and safety properties of nano-LFP has spurred interest in finding other phosphates that might have much higher energy densities. One approach is to use materials that can incorporate up to two lithium ions. One such material is $VOPO_4$, which must be nanosized and carbon coated to be operative[109], but has the advantage of being made of relatively abundant materials[47,66]. This material forms Li_2VOPO_4 (LVP) on discharge and has a capacity of 305 Ah/kg compared to the 170 Ah/kg of LFP. However, the lifetime and stability are inadequate for EV use and much work is still needed to make LVP commercially viable.

Spinel $LiMn_2O_4$ (LMO) is made of abundant manganase[47,66], is relatively safe to handle[86,110], and has relatively low damages associated with its production[50,51]. Nanosized spinel LMO has been synthesized in various morphologies. Studies have found increased power densities[47], and although increased energy densities have also been obtained[107], these are not as high as those of bulk NMC and NCA[47,106]. In the case of LMO, nanoparticles tend to increase the undesirable dissolution of manganese to the electrolyte[32,107], leading to lifetime issues. Porous nanorods, however, have been found to have remarkable lifetime[111].

As one of very few viable options to the intercalation materials, the conversion material sulphur has received intense interest in the past decade due to exceptionally high theoretical energy density[112–115]. Supply of sulphur is unlikely to become an issue as it is the thirteenth most abundant element in the earth's crust[47]. In batteries, the insulating nature of sulphur results in poor power density and creates large internal resistance and polarization of the battery[116], resulting in poor device efficiency. Furthermore, volume expansion (~80%) and dissolution of intermediate reaction products (polysulphides) in the electrolyte result in poor lifetime[47,113]. The most promising approach to mitigate poor conductivity and lifetime is the encapsulation of sulphur within conductive additives to form sulphur-carbon and sulphur-polymer nanocomposites[47,117]. Sulphur-carbon nanocomposites pose higher exposure risks and hazards[56,118] than sulphur nanocomposites with polymers such as polyacrylonitrile, polyvinylpyrrolidone, polydimethylsiloxane[118,119], and polyaniline[118,120]. Even if the issue of lifetime is overcome, the sulphur cathode must be paired with a lithium metal or a lightweight lithiated anode for high energy density[47,114,121,122]. In contrast, lithium sulphide (Li_2S), can be paired with lithium-free anodes, which avoids safety concerns and short lifetime[122]. Although the Li_2S cathode has a high theoretical capacity, it is both electronically and ionically insulating[47], which have led to various efforts using conductive additives, such as metals and carbon[114]. Earlier studies tended to focus on Li_2S-metal composites, but the inherent disadvantages of Li_2S-metal composites have created extensive interest in the development and use of Li_2S-carbon composites in the past five years[116]. Due to a high content of lithium and carbon nanostructures, care should be taken when handling nanostructured Li_2S-carbon composites[56,86]. Studies have reported different nanostructures, synthesis methods, and carbon content in Li_2S-carbon nanocomposites and this can lead to significant differences in material losses and energy use, which in turn influence greenhouse gas emissions and damages to human health and ecosystems. Further improvement on lifetime is required for Li_2S cathode materials to replace the layered oxides from the EV market.

Recycling of LIBs

There are several competing industrial LIB recycling processes[123]. LIB recycling is typically a combination of two or more of the following processes: mechanical separation, pyrometallurgical, and hydrometallurgical treatment. The various industrial recycling pathways offer different yields depending on the recycling route and electrode materials. As the metal value in batteries is mainly driven by prices of cobalt and nickel metals, current recycling processes still focus on the recovery of these metals[97,124,125]. Other transition metals, such as copper and iron, are also typically recovered in the current industrial LIB recycling processes. In only a few recycling routes are aluminium, lithium, and manganese recovered[97,123,125]. According to relevant literature[97,123,126] and personal communication with two European recycling companies[127,128], phosphate and graphite are normally not recycled in current industrial processes. Nanostructured LFP is currently recycled successfully[127], which may suggest that nanostructuring electrode materials do not affect recycling yields compared to bulk materials. During recycling, however, nanomaterials may become airborne, which can pose exposure risk and hazard to workers[129].

5. Nanotechnologies in fuel cell developments

While there are multiple fuel cell types, we focus here on PEMFCs, which demonstrate the most potential within the transport sector[10,15,21]. High cost, durability and lifetime challenges are all barriers to the mainstream adoption of fuel cell EVs[27]; in contrast to battery EVs, commercial sale of fuel cell EVs has only very recently become reality[130,131]. In contrast to LIBs, the ’baseline’ materials are already in nanoform; we review here rather alternative nanostructures and nanomaterials that have the potential to replace current state of the art materials. These advances in nanotechnology have shown promising opportunities to improve the technical and environmental performance of PEMFCs in EVs and thus encourage their widespread commercial adoption.

Figures 4 and 5 summarize the lifecycle attributes of some of the most promising nanostructured materials for cathode catalyst and catalyst support, respectively. Although the electrocatalyst often refers to the catalyst and support together (Pt/C), they are considered as two components independent of each other in this study. Electrolyte membranes, being a bulk material, are discussed in section 4 of the Supplementary Information while nanotechnological improvements to these bulk materials are discussed in the text. .

Cathode catalysts

The oxygen reduction reaction occurring at the cathode is enabled by the cathode catalyst; a well-performing catalyst is therefore a determinant of the device’s overall power output. At present, both PEMFC anodes and cathodes rely on platinum catalysts supported on high surface area carbon (Pt/C), which are costly, scarce[47] and have extremely high environmental implications from platinum extraction[50,51]. In terms of efficient use of this high-impact, non-renewable material, the cathode is the key technological bottleneck as the oxygen reduction reaction occurs five to six orders of magnitude slower than the hydrogen oxidation reaction occurring at the anode[28], thus greatly limiting the cell power density. Furthermore, the pure platinum catalysts suffer from poisoning from impurities in the hydrogen fuel as well as dissolution and agglomeration, which can drastically shorten the fuel cell lifetime[29,132,133]. A shorter lifetime demands more frequent replacement of PEMFC stacks in EVs, and may ultimately require more platinum extraction per kilometre driven. Current research therefore focuses on reducing or eliminating platinum use in the catalyst[134–136]. Several solutions are being explored, including the use of ultra-low platinum loading, platinum alloys and platinum-free catalysts to reduce material costs while maintaining or improving catalytic activity over current Pt/C catalysts. In comparison to the commercial Pt/C catalyst, most of these platinum-containing alternatives yield enhanced durability (Figure 4) and demonstrate similar or superior oxygen reduction reaction catalytic ability.

Alternative platinum nanomorphologies and nanostructured platinum alloys can maintain or even increase the catalytic activity relative to conventional Pt/C catalysts. Increasing the specific catalytic activity allows for a reduction in the amount of platinum used, thus improving material efficiency over the conventional catalyst. In addition to the various nanomorphologies, research using different assembly methods, such as electrospraying, improve catalytic activity by influencing the hierarchical structure of the electrode[137,138]. Similarly, platinum alloys with nickel[139–141], cobalt[140,142] and copper[143,144] have also demonstrated good performance while decreasing platinum use.

While platinum reduction is a desirable goal for PEMFC development, the complete elimination of platinum use in PEMFCs would be an even greater improvement of the material environmental impacts [66,145]. Non-precious metal catalysts using more abundant metals such as iron have been tested, but present severely depressed technical performance and stability in acidic operating conditions[146]. Other metal catalysts based on niobium, tantalum, and zirconium have improved lifetime over Pt/C, but do not meet power density expectations, and are more scarce[47,66] and environmentally intensive to produce than iron[50,51], although they still represent an improvement over platinum. Metal-free catalysts using functionalized carbon nanostructures, particularly N-doped carbon nanotubes and graphene materials, are promising candidates for platinum-free catalysts that capitalize on abundant precursor materials, though they require further research to improve the energy efficiency of their synthesis and to provide adequate catalytic ability in acidic environments[147–149]. A clear trend, however, is that platinum-free catalysts continue to struggle in catalytic activity and lifetime in comparison to low-platinum and platinum-alloy catalysts[147].

In addition to the morphological and material nature of the catalyst, the hierarchical organization of the nanostructured materials in the device also affects catalyst performance. While such organization may increase material efficiency by increasing catalytic activity, it may also present consequential side issues such as water flooding, which in turn cancels out or exceeds the gains in performance, or causes unstable cell performance[150].

If the goal is to reduce the amount of platinum used in fuel cell EVs to the amount used in the catalytic converters of conventional internal combustion engine vehicles, the device lifetime must be accounted for. Since fuel cell EVs currently have a shorter lifetime than conventional vehicles, the amount of platinum required to drive an equal distance increases, i.e., several fuel cell stacks will be required. Furthermore, the growing light-duty vehicle market represents an unsustainable demand for further platinum extraction into the future. Rather, focus should be placed on robust, low- or non-platinum catalysts with long lifetime.

Cathode catalyst supports

Effective support materials enhance catalytic catalyst utilization and thus increase material efficiency by allowing for smaller quantities of catalyst while maintaining similar levels of catalytic activity. A catalyst support would ideally maximize the catalyst surface area available for reactions and maintain high electric conductivity for high energy efficiency. Supports made of carbon black currently used in commercial PEMFC catalysts are vulnerable to corrosion, which causes catalyst sintering and decreases the amount of conductive material in the electrode, thereby decreasing power density and PEMFC lifetime[29,151]. Carbon black-based support materials also suffer from deep micropores that physically block reagent access to the catalyst and thus decrease catalyst efficiency[152].

Nanostructured materials can provide the characteristics needed for an effective catalyst support, including a high surface area with a mesoporous structure that does not inhibit catalytic activity[153]. Catalyst support materials must also be sufficiently electrically conductive in order to reduce internal resistance, thereby enhancing charge transport within the cell and be stable at higher temperatures and in the acidic environment of a PEMFC.

The two most promising catalyst support materials that are environmentally beneficial and demonstrate improved technical performance are carbon nanostructures and titanium dioxide, two materials with low environmental intensity in their bulk form[50,51] (Figure 5). The synthesis methods for the nanomorphologies, however, may potentially have high energy demand[60], and thereby be detrimental to the overall climate change performance of the manufacturing process. The graphitized carbon-based nanomaterials have enhanced durability under fuel cell operating conditions[29], which improves the climate change performance of the PEMFC over the lifetime as a counterpoint for the increased synthesis energy. Doping the carbon with heteroatoms such as nitrogen, phosphorus or sulphur functionalizes the otherwise inert carbon to allow catalyst deposition[152]. In some cases, functionalization, such as with nitrogen-doped carbon nanotubes, also allows the otherwise catalytically inert carbon supports to become catalytically active, thereby increasing power density of the PEMFC[154]. Some carbon-polymer nanocomposites have shown improved material efficiency via power density, but, in some cases, this is in exchange for reduced lifetime.

Carbon-free, transition metal oxide-based supports such as titanium dioxide in mesoporous or nanofiber morphologies, while relatively robust, have not yet achieved the same performance level as the baseline carbon black catalyst support. Composite titanium dioxide catalyst supports may also be more sensitive to scarcity[47,66] and material production impacts[50,51] than carbon-based supports, as are supports of niobium- and ruthenium oxide-doped titanium dioxide.

Electrolyte membrane

The PEMFC membrane, with its high cost[155], poor durability[29] and intolerance to fuel impurities[156], represents another obstacle to the widespread commercialization of transport PEMFCs. The current commercial baseline, Nafion®, is a perfluorinated membrane that performs poorly in temperatures beyond 80 °C and in low-humidity environments, and is not stable with impure feed gases[157,158]. An ideal membrane for transport PEMFCs must therefore have satisfactory performance and stability at these conditions. Research has been directed towards more robust membranes, which would allow for thinner membranes that represent an improvement in material efficiency (less membrane material used) and device efficiency (e.g., superior ion exchange/proton conductivity performances). While membrane polymers conduct protons at the nanoscale, the membrane material itself does not constitute a nanomaterial. A brief review of the main membrane polymer groups may be found in Section 4 in the Supplementary information. Nanotechnology offers several options for improving these bulk membranes. Such options include the use of nanofillers to enhance the membrane, or the use of nanosynthesis methods to provide a superior hierarchical structure to the membrane.

One attractive strategy of generating an optimum balance between ion conduction and physicochemical stability in electrolyte membranes is to create a "microphase-separated" morphology in polymers made of highly ordered ion-nanochannels and a hydrophobic phase. An example is the fabrication of ion-conductive polymer nanofibers, demonstrating distinctive electrochemical, physicochemical, and thermal properties owing to their high specific surface area and polymer orientation along the nanofiber direction[159,160]. The use of a reinforcing, mechanically strong nanofiber morphology can minimize in-plane swelling changes during wet(on)/off(-dry) fuel cell operation and thus extend the device lifetime[161]. Some success has been achieved with a dual electrospun composite of poly(phenyl sulfone) and Nafion[162], where PPSU provides mechanical stability to the PFSA membrane, thus improving lifetime while maintaining device efficiency (cell power output). Similarly, improved proton conductivity, leading to increased power density was achieved with electrospun acid-doped polybenzimidazole in a sulfonated polymer matrix in comparison to a similar composite membrane without nanofiber morphology[160].

In one type of composite membrane, a polymer membrane matrix may have embedded nanostructures of inorganic materials in order to improve membrane characteristics. Such materials may be metal oxides or synthetic clays to improve mechanical stability[163], water uptake, or nanocarbons or nanofibers to provide ionic channels and thus improve device efficiency of the PEMFC. Heteropolyacids such as phosphotungtsic acid are used as fillers to improve proton conductivity (device efficiency), but decease mechanical stability and therefore have a shorter lifetime. Phosphotungstic acid also has significant exposure risks[164]. However, while hygroscopic particles are intended to increase the device efficiency by improving proton conductivity via increased water retention, these particles decrease device efficiency by diluting the concentration of the proton-conducting ionomer when made of material less conductive that the ionomer membrane[165–168]. Nanofillers may also increase the mechanical strength of the polymer, as in the case of zwitterionic structured SiO_2 in polybenzimidazole[163,169]. In addition, the heterogeneous hybrid membranes also experience phase separation due to differing water uptake and thermal expansion coefficients of the nanofillers and the polymer matrix, causing stresses and strains in the membrane and thereby shortening the lifetime and decreasing material efficiency[170].

Hierarchical ordering in these nanocomposites are also a promising strategy to improve membrane performance; in particular, the alignment of one-dimensional (nanotubes, nanofibers or nanorods) and two-dimensional nanomaterials (nanoflakes, nanosheets, or nanoplates) in the membrane have a two-fold benefit. In the direction parallel to the membrane, proton conductivity is improved, while the across the membrane, mechanical properties, chemical stability and fuel permeability characteristics are improved. Graphene oxide[173] and electrospun[160,162] nanofibers are particularly emphasized due to the creation of long-range ordered ionic nanochannels for proton conduction and excellent physicochemical stability.

Recycling of PEMFCs

In terms of both cost and environmental intensity, platinum catalyst and fluorinated membranes are of greatest interest for recycling and recovery processes. The most common platinum recovery approaches include selective chlorination or gas phase volatilization, hydrometallurgical and pyrometallurgical processes[171]. Selective chlorination or gas phase volatilization, however, require carbon monoxide and chlorine gases or aggressive solvents such as aqua regia or cyanide. Many of these compounds pose considerable risks to workers[172–174]. Many hydrometallurgical approaches also require high operating temperatures and pressures, making them energy intensive processes. Pyrometallurgical processes for PEMFCs containing fluorinated membranes such as Nafion would result in the emission of highly toxic hydrogen fluoride[175,176]. The Pt/C catalyst can also be recovered using a chemical recovery process after carbon-based supports are incinerated[175,176]. Generally, alloying and non-combustible elements consisting of 10% or less of the total recoverable materials will not detrimentally affect recoverability or reusability of precious metal catalysts[128].

Mechanical separation of membranes from the catalyst layers is difficult, as these components are generally hot-pressed together[175]. Re-use of the membrane is also unlikely as performance drops in fuel cells are usually caused by membrane degradation or failure due to dehydration and pin-holing, which makes recycling a more likely end-of-life fate for membranes[175]. Nafion membranes are generally recovered using chemical extraction[175–177], after which a new membrane may be re-cast, although possibly with some loss of quality[177]. As with the catalyst, it is unknown whether the adoption of novel multi-element catalysts and alternative catalyst support materials in PEMFCs will affect the yield or quality of recovered precious metals given the current PEMFC recycling techniques.

6. The road ahead

Nanomaterials are opening a broad range of opportunities to improve the technical and lifecycle environmental performance of EVs. Identifying the alternative material candidates with the most promising opportunities for enhancing overall environmental performance of LIBs and PEMFCs in EVs at an early stage is therefore important. To this end, we performed an early stage lifecycle environmental screening and mapped their potential strengths and weaknesses with respect to key lifecycle attributes (Figures 2-5). We found that no single nanomaterial seems poised to outcompete its rivals in terms of all reviewed sustainability criteria for any of the reviewed LIB and PEMFC materials. Rather, the current research frontier presents multiple promising candidates for continued development, each subject to non-trivial environmental trade-offs that should be addressed.

To maximize climate change mitigation benefits offered by EVs, we must improve both the electrochemical and environmental performance of LIBs and PEMFCs. Nanomaterials show great promise in providing the necessary technical breakthrough in these devices, but their ability to be a part of the mitigation solution for transport-related greenhouse gas emissions depends on several life cycle attributes spanning from extraction, refinement, synthesis, operational performance, durability and recyclability. As such, the next generation of LIBs and PEMFCs should ideally be based on abundant resources that can be extracted and refined with low energy consumption and environmental impacts. It should be resource and material efficient, achieved through improvements in synthesis yields, lightweighting, durability and ultimately, recyclability. Finally, it should be energy efficient, both in the production and use phase. In practice though, we are likely have to make some trade-offs. Our analysis of the current situation clearly outlines the challenge: the materials with the best potential environmental profiles during the material extraction and production phase (less environmentally intensive materials, lower nanosynthesis energy use, and facile synthesis) often present environmental disadvantages during their use-phase (lower energy efficiency, heavier battery, or shorter lifetimes), and vice versa.

Meeting this challenge will require concerted efforts and a new focus within the nanotechnology community. Throughout this review, we found that publications on novel nanomaterials rarely explicitly communicate synthesis yields, solvent use, and energy consumption during production. These are all are key parameters that significantly influence the environmental performance and that can largely be improved through the choice of alternative synthesis protocols and foreseeable economies of scale. Improved, systematic and consistent reporting of these attributes would remove a very avoidable source of uncertainty. Improved flow of information would be of mutual benefit to both the LCA and nanotechnology communities; through joint efforts, both communities would be able to direct research efforts towards the materials and synthesis protocols with the best environmental sustainability potential. An extension of the above aspect is the current lack of data regarding potential toxic effects, which unfortunately remain a challenge for nearly all of the investigated nanomaterials. Similarly, we also found little literature on how the physicochemical properties of novel nanomaterials affect existing recycling and disposal processes. Addressing these issues would over time allow us to efficiently manoeuver towards the most environmentally superior options. As more detailed and consistent information becomes available, one can move from screening studies to detailed LCAs in order to refine our understanding and ultimately make the right design tradeoffs that optimize LIB and PEMFC nanomaterials for EV usage towards mitigating climate change. This will require a cross-disciplinary collaboration between material scientists and LCA practitioners to reap – and maximize – the benefits offered by simultaneously incorporating nanotechnology, nanotoxicology, eco-design and green chemistry considerations. If we succeed, nanotechnology can be a key contributor to climate change mitigation in the transport sector.

References

1. Gabriel, B. *et al.* in *Climate Change 2014: Mitigation of Climate Change. Contribution of Working Group III to the Fifth Assessment Report of the Intergovernmental Panel on Climate Change* (eds. Edenhofer, O. et al.) 351–412 (Cambridge University Press, 2014).
2. Sims, R. *et al.* in *Climate Change 2014: Mitigation of Climate Change. Contribution of Working Group III to the Fifth Assessment Report of the Intergovernmental Panel on Climate Change* (ed. Edenhofer, O., R. Pichs-Madruga, Y. Sokona, E. Farahani, S. Kadner, K. Seyboth, A. Adler, I. Baum, S. Brunner, P. Eickemeier, B. Kriemann, J. Savolainen, S. Schlömer, C. von Stechow, T. Z. and J. C. M.) 1–115 (Cambridge University Press, 2014).
3. Shepard, S. & Jerram, L. *Executive Summary: Transportation Forecast : Light Duty Vehicles*. (2015).
4. International Energy Agency. *Global EV Outlook 2016 Beyond one million electric cars*. (2016).
5. European Automobile Manufacturers' Association. Overview of purchase and tax incentives for electric vehicles in the EU. 1–7 (2016).
6. Crabtree, G., Kócs, E. & Trahey, L. The energy-storage frontier: Lithium-ion batteries and beyond. *MRS Bull.* **40,** 1067–1078 (2015).
7. Samaras, C. & Meisterling, K. Life cycle assessment of greenhouse gas emissions from plug-in hybrid vehicles: implications for policy. *Environ. Sci. Technol.* **42,** 3170–6 (2008).
8. Szczechowicz, E., Dederichs, T. & Schnettler, A. Regional assessment of local emissions of electric vehicles using traffic simulations for a use case in Germany. *Int. J. Life Cycle Assess.* **17,** 1131–1141 (2012).
9. Helmers, E. & Marx, P. Electric cars: technical characteristics and environmental impacts. *Environ. Sci. Eur.* **24,** 14 (2012).

10. Simons, A. & Bauer, C. A life-cycle perspective on automotive fuel cells. *Appl. Energy* **157,** 884–896 (2015).

11. Hellweg, S. & Milà i Canals, L. Emerging approaches, challenges and opportunities in life cycle assessment. *Science* **344,** 1109–13 (2014).

12. Kushnir, D. & Sandén, B. a. Energy requirements of carbon nanoparticle production. *J. Ind. Ecol.* **12,** 360–375 (2008).

13. Kushnir, D. & Sandén, B. a. Multi-level energy analysis of emerging technologies: A case study in new materials for lithium ion batteries. *J. Clean. Prod.* **19,** 1405–1416 (2011).

14. Bartolozzi, I., Rizzi, F. & Frey, M. Comparison between hydrogen and electric vehicles by life cycle assessment: A case study in Tuscany, Italy. *Appl. Energy* **101,** 103–111 (2013).

15. Bauer, C., Hofer, J., Althaus, H.-J., Del Duce, A. & Simons, A. The environmental performance of current and future passenger vehicles: Life Cycle Assessment based on a novel scenario analysis framework. *Appl. Energy* 1–13 (2015). doi:10.1016/j.apenergy.2015.01.019

16. Dunn, J. B., Gaines, L., Kelly, J. C., James, C. & Gallagher, K. G. The significance of Li-ion batteries in electric vehicle life-cycle energy and emissions and recycling's role in its reduction. *Energy Environ. Sci.* **8,** 158–168 (2015).

17. Faria, R., Moura, P., Delgado, J. & de Almeida, A. T. A sustainability assessment of electric vehicles as a personal mobility system. *Energy Convers. Manag.* **61,** 19–30 (2012).

18. Ellingsen, L. A.-W., Singh, B. & Strømman, A. H. The size and range effect: lifecycle greenhouse gas emissions of electric vehicles. *Environ. Res. Lett.* **11,** (2016).

19. Hawkins, T. R., Singh, B., Majeau-Bettez, G. & Strømman, A. H. Comparative Environmental Life Cycle Assessment of Conventional and Electric Vehicles. *J. Ind. Ecol.* **17,** 53–64 (2012).

20. Miotti, M., Hofer, J. & Bauer, C. Integrated environmental and economic assessment of current and future fuel cell vehicles. *Int. J. Life Cycle Assess.* (2015). doi:10.1007/s11367-015-0986-4

21. Notter, D. A., Kouravelou, K., Karachalios, T., Daletou, M. K. & Haberland, N. T. Life cycle assessment of PEM FC applications: electric mobility and μ-CHP. *Energy Environ. Sci.* **8,** 1969–1985 (2015).

22. Notter, D. A. *et al.* Contribution of Li-ion batteries to the environmental impact of electric vehicles. *Environ. Sci. Technol.* **44,** 6550–6 (2010).

23. Li, B., Gao, X., Li, J. & Yuan, C. Life Cycle Environmental Impact of High-Capacity Lithium Ion Battery with Silicon Nanowires Anode for Electric Vehicles. *Environ. Sci. Technol.* **48,** 3047–3055 (2014).

24. Majeau-Bettez, G., Hawkins, T. R. & Strømman, A. H. Life cycle environmental assessment of lithium-ion and nickel metal hydride batteries for plug-in hybrid and battery electric vehicles. *Environ. Sci. Technol.* **45,** 4548–54 (2011).

25. Zackrisson, M., Avellan, L. & Orlenius, J. Life cycle assessment of lithium-ion batteries for plug-in hybrid electric vehicles - Critical issues. *J. Clean. Prod.* **18,** 1519–1529 (2010).

26. Singh, B., Guest, G., Bright, R. M. & Strømman, A. H. Life Cycle Assessment of Electric and Fuel Cell Vehicle Transport Based on Forest Biomass. *J. Ind. Ecol.* **18,** (2014).

27. Othman, R., Dicks, A. L. & Zhu, Z. Non precious metal catalysts for the PEM fuel cell cathode. *Int. J. Hydrogen Energy* **37,** 357–372 (2012).

28. Debe, M. K. Electrocatalyst approaches and challenges for automotive fuel cells. *Nature* **486,** 43–51 (2012).

29. Wu, J. *et al.* A review of PEM fuel cell durability: Degradation mechanisms and mitigation strategies. *J. Power Sources* **184,** 104–119 (2008).

30. Shiau, C.-S. N., Samaras, C., Hauffe, R. & Michalek, J. J. Impact of battery weight and charging patterns on the economic and environmental benefits of plug-in hybrid vehicles. *Energy Policy* **37,** 2653–2663 (2009).

31. Iwan, A., Malinowski, M. & Pasciak, G. Polymer fuel cell components modified by graphene: Electrodes, electrolytes and bipolar plates. *Renew. Sustain. Energy Rev.* **49,** 954–967 (2015).

32. Aricò, A. S., Bruce, P., Scrosati, B., Tarascon, J.-M. & van Schalkwijk, W. Nanostructured materials for advanced energy conversion and storage devices. *Nat. Mater.* **4,** 366–377 (2005).

33. Bruce, P. G., Scrosati, B. & Tarascon, J.-M. Nanomaterials for rechargeable lithium batteries. *Angew. Chem. Int. Ed. Engl.* **47,** 2930–2946 (2008).

34. Goriparti, S. *et al.* Review on recent progress of nanostructured anode materials for Li-ion batteries. *J. Power Sources* **257,** 421–443 (2014).

35. Nie, Y., Li, L. & Wei, Z. Recent advancements in Pt and Pt-free catalysts for oxygen reduction reaction. *Chem. Soc. Rev.* **44,** 2168–201 (2015).

36. Whittingham, M. S. Inorganic nanomaterials for batteries. *Dalt. Trans.* 5424–5431 (2008). doi:10.1039/b805658g

37. Whittingham, M. S. Ultimate limits to intercalation reactions for lithium batteries. *Chem. Rev.* **114,** 11414–43 (2014).

38. Obrovac, M. N. & Chevrier, V. L. Alloy Negative Electrodes for Li-Ion Batteries. *Chem. Rev.* **114,** 141117082517000 (2014).

39. Liu, C., Li, F., Ma, L.-P. & Cheng, H.-M. Advanced materials for energy storage. *Adv. Mater.* **22,** E28–E62 (2010).

40. Gallagher, K. G. *et al.* Quantifying the promise of lithium–air batteries for electric vehicles. *Energy Environ. Sci.* **7,** 1555 (2014).

41. Graedel, T. E., ALLENBY, B. R. & COMRIE, P. R. Matrix Approaches to Abridged Life Cycle Assessment. *Environ. Sci. Technol.* **29,** 134A–139A (1995).

42. Graedel, T. E. *Streamlined life-cycle assessment*. (Prentice Hall, 1998).

43. Todd, J. A. *et al.* Streamlined Life-Cycle Assessment: A Final Report from the SETAC North America Streamlined LCA Workgroup. *Environ. Toxicol.* 31 (1999).

44. Anastas, P. T. & Warner, J. C. *Green Chemistry: Theory and Practice*. (Oxford University Press, 1998).

45. Anastas, P. T. & Eghbali, N. Green Chemistry: Principles and Practice. *Chem. Soc. Rev.* **39,** 301–312 (2010).

46. Ellingsen, L. A.-W. *et al.* Life cycle assessment of a lithium-ion battery vehicle pack. *J. Ind. Ecol.* **18,** 113–124 (2014).

47. Nitta, N., Wu, F., Lee, J. T. & Yushin, G. Li-ion battery materials: present and future. *Mater. Today* **18,** 252–264 (2015).

48. Whittingham, M. S. History, Evolution, and Future Status of Energy Storage. *Proc. IEEE* **100,** 1518–1534 (2012).

49. Yoshino, A. in *Lithium-Ion Batteries* 1–20 (Elsevier, 2014). doi:10.1016/B978-0-444-59513-3.00001-7

50. ReCiPe. ReCiPe Mid/Endpoint method, version 1.11. (2015).

51. Ecoinvent Centre. *Ecoinvent data and reports 3.2*. (2015).

52. Hudak, N. S. in *Lithium-Ion Batteries: Advances and Applications* (ed. Pistoia, G.) 57–82 (Elsevier, 2014). doi:10.1016/B978-0-444-59513-3.00004-2

53. Ohta, N., Nagaoka, K., Hoshi, K., Bitoh, S. & Inagaki, M. Carbon-coated graphite for anode of lithium ion rechargeable batteries: Graphite substrates for carbon coating. *J. Power Sources* **194,** 985–990 (2009).

54. Latorre-Sanchez, M., Primo, A. & Garcia, H. Green synthesis of Fe3O4 nanoparticles

embedded in a porous carbon matrix and its use as anode material in Li-ion batteries. *J. Mater. Chem.* **22,** 21373 (2012).

55. Lahiri, I. & Choi, W. Carbon Nanostructures in Lithium Ion Batteries: Past, Present, and Future. *Crit. Rev. Solid State Mater. Sci.* **38,** 128–166 (2013).

56. US Research Nanomaterials Inc. Safety data sheet - carbon nanostructures. (2015).

57. ESPI Metals. Material Safety Data Sheets. Available at: http://www.espimetals.com/index.php/msds.

58. Kim, H. C. & Fthenakis, V. Life Cycle Energy and Climate Change Implications of Nanotechnologies. *J. Ind. Ecol.* **17,** 528–541 (2013).

59. Gutowski, T. G. *et al.* Thermodynamic analysis of resources used in manufacturing processes. *Environ. Sci. Technol.* **43,** 1584–1590 (2009).

60. Şengül, H., Theis, T. L. & Ghosh, S. Toward Sustainable Nanoproducts. *J. Ind. Ecol.* **12,** 329–359 (2008).

61. De Volder,Michael F. L. Sameh H. Tawfick, R. H. B. and & Hart, A. J. Carbon Nanotubes : Present and Future Commercial Applications. *Science (80-.).* **339,** 535–539 (2013).

62. Charitidis, C. a., Georgiou, P., Koklioti, M. a., Trompeta, A.-F. & Markakis, V. Manufacturing nanomaterials: from research to industry. *Manuf. Rev.* **1,** 11 (2014).

63. Sharifi, S. *et al.* Toxicity of nanomaterials. *Chem. Soc. Rev.* **41,** 2323–43 (2012).

64. Bystrzejewska-Piotrowska, G., Golimowski, J. & Urban, P. L. Nanoparticles: Their potential toxicity, waste and environmental management. *Waste Manag.* **29,** 2587–2595 (2009).

65. Köhler, A. R., Som, C., Helland, A. & Gottschalk, F. Studying the potential release of carbon nanotubes throughout the application life cycle. *J. Clean. Prod.* **16,** 927–937 (2008).

66. Graedel, T. E., Harper, E. M., Nassar, N. T., Nuss, P. & Reck, B. K. Criticality of metals and metalloids. *Proc. Natl. Acad. Sci.* **112,** 4257–4262 (2015).

67. Lee, W. W. & Lee, J.-M. Novel synthesis of high performance anode materials for lithium-ion batteries (LIBs). *J. Mater. Chem. A* **2,** 1589–1626 (2014).

68. Reddy, M. V, Subba Rao, G. V & Chowdari, B. V. Metal oxides and oxysalts as anode materials for Li ion batteries. *Chem Rev* **113,** 5364–5457 (2013).

69. Ma, Y., Ding, B., Ji, G. & Lee, J. Y. Carbon-Encapsulated F-Doped Li4Ti5O12 as a high rate anode material for Li+ Batteries. *ACS Nano* **7,** 10870–10878 (2013).

70. Anderman, M. *The Tesla Battery Report*. (Total Battery Consulting, Inc, 2016).

71. NEI Corporation. Safety Data Sheet - Lithium Titanium Oxide. 1–6 (2014).

72. Gan, L. *et al.* A facile synthesis of graphite/silicon/graphene spherical composite anode for lithium-ion batteries. *Electrochim. Acta* **104,** 117–123 (2013).

73. Zamfir, M. R., Nguyen, H. T., Moyen, E., Lee, Y. H. & Pribat, D. Silicon nanowires for Li-based battery anodes: a review. *J. Mater. Chem. A* **1,** 9566–9586 (2013).

74. Scrosati, B. & Garche, J. Lithium batteries: Status, prospects and future. *J. Power Sources* **195,** 2419–2430 (2010).

75. Su, X. *et al.* Silicon-Based Nanomaterials for Lithium-Ion Batteries: A Review. *Adv. Energy Mater.* **4,** 1–23 (2014).

76. Ge, M., Rong, J., Fang, X. & Zhou, C. Porous doped silicon nanowires for lithium ion battery anode with long cycle life. *Nano Lett.* **12,** 2318–2323 (2012).

77. Jia, H. *et al.* Novel three-dimensional mesoporous silicon for high power lithium-ion battery anode material. *Adv. Energy Mater.* **1,** 1036–1039 (2011).

78. US Research Nanomaterials Inc. Safety Data Sheet - Silicon Nanopowder / Nanoparticles. (2016).

79. Sigma Aldrich. Material Safety Data Sheet - Monodispersed silicon nanowires. (2010).

80. American Elements. Safety Data Sheet - Tin Oxide Nanopowder. (2015).

81. US Research Nanomaterials Inc. Material Safety Data Sheet - Germanium Nanoparticles.

82. Dong, Z. *et al.* The Anode Challenge for Lithium-Ion Batteries: A Mechanochemically Synthesized Sn-Fe-C Composite Anode Surpasses Graphitic Carbon. *Adv. Sci.* **3,** 1–8 (2016).

83. Sony Global - News Release - SONY's NEW NEXELION HYBRID LITHIUM ION BATTERIES. Available at: http://www.sony.net/SonyInfo/News/Press/200502/05-006E/. (Accessed: 21st November 2015)

84. Fan, Q., Chupas, P. J. & Whittingham, M. S. Characterization of Amorphous and Crystalline Tin–Cobalt Anodes. *Electrochem. Solid-State Lett.* **10,** A274 (2007).

85. American Elements. Safety Data Sheet - Iron(II,III) Oxide Nanopowder. (2015).

86. LTS Chemical. SDS | LTS. Available at: https://www.ltschem.com/msds/. (Accessed: 22nd April 2016)

87. US Research Nanomaterials Inc. Material Safety Data Sheet - Cobalt (II) Oxide Nanoparticles (CoO).

88. American Elements. *Safety Data Sheet - Chromium Oxide Nanopowder*. (2015).

89. American Elements. *Safety Data Sheet - Molybdenum Oxide Nanopowder*. (2015).

90. Wang, B., Chen, J. S., Wu, H. B., Wang, Z. & Lou, X. W. Quasiemulsion-templated formation of alpha-Fe2O3 hollow spheres with enhanced lithium storage properties. *J. Am. Chem. Soc.* **133,** 17146–17148 (2011).

91. Etacheri, V., Marom, R., Elazari, R., Salitra, G. & Aurbach, D. Challenges in the development of advanced Li-ion batteries: a review. *Energy Environ. Sci.* **4,** 3243–3262 (2011).

92. Li, Q. *et al.* Balancing stability and specific energy in Li-rich cathodes for lithium ion batteries: a case study of a novel Li–Mn–Ni–Co oxide. *J. Mater. Chem. A* **3,** 10592–10602 (2015).

93. Rosenman, A. *et al.* Review on Li-Sulfur Battery Systems: An Integral Perspective. *Adv. Energy Mater.* **5,** 1–21 (2015).

94. Bruce, P. G., Freunberger, S. a., Hardwick, L. J. & Tarascon, J.-M. Li–O2 and Li–S batteries with high energy storage. *Nat. Mater.* **11,** 172–172 (2011).

95. American Elements. Safety Data Sheet - Lithium Cobalt Oxide Nanopowder. (2015).

96. Whittingham, M. S. Lithium batteries and cathode materials. *Chem. Rev.* **104,** 4271–4301 (2004).

97. Hanisch, C., Diekmann, J., Stieger, A., Haselrieder, W. & Kwade, A. Recycling of Lithium-Ion Batteries. *Handb. Clean Energy Syst.* 1–24 (2015). doi:10.1002/9781118991978.hces221

98. NEI Corporation. *Material Safety Data Sheet - Lithium Manganese Nickel Cobalt Oxide powder*. (2014).

99. NEI Corporation. *Safety Data Sheet - Lithium Nickel Cobalt Aluminum Oxide*. (2014).

100. Liu, J., Wang, R. & Xia, Y. Degradation and Structural Evolution of xLi2MnO3{middle dot}(1-x)LiMn1/3Ni1/3Co1/3O2 during Cycling. *J. Electrochem. Soc.* **161,** A160–A167 (2013).

101. Pfaltz & Bauer. Safety data sheet - LMR. 1–5 (2013).

102. Yu, H. & Zhou, H. High-Energy Cathode Materials (Li 2 MnO 3 –LiMO 2) for Lithium-Ion Batteries. *J. Phys. Chem. Lett.* **4,** 1268–1280 (2013).

103. Liu, J. *et al.* General synthesis of xLi2MnO3·(1 − x)LiMn1/3Ni1/3Co1/3O2 nanomaterials by a molten-salt method: towards a high capacity and high power cathode for rechargeable lithium batteries. *J. Mater. Chem.* **22,** 25380 (2012).

104. Croy, J. R., Balasubramanian, M., Gallagher, K. G. & Burrell, A. K. Review of the U.S. Department of Energy's 'deep Dive' Effort to Understand Voltage Fade in Li- and Mn-Rich Cathodes. *Acc. Chem. Res.* **48,** 2813–2821 (2015).

105. Ellis, B. L., Lee, K. T. & Nazar, L. F. Positive Electrode Materials for Li-Ion and Li-Batteries [†]. *Chem. Mater.* **22,** 691–714 (2010).

106. Pampal, E. S., Stojanovska, E., Simon, B. & Kilic, A. A review of nanofibrous structures in lithium ion batteries. *J. Power Sources* **300,** 199–215 (2015).

107. Song, M. K., Park, S., Alamgir, F. M., Cho, J. & Liu, M. Nanostructured electrodes for lithium-ion and lithium-air batteries: The latest developments, challenges, and perspectives. *Mater. Sci. Eng. R Reports* **72,** 203–252 (2011).

108. Satyavani, T. V. S. L., Srinivas Kumar, A. & Subba Rao, P. S. V. Methods of synthesis and performance improvement of lithium iron phosphate for high rate Li-ion batteries: A review. *Eng. Sci. Technol. an Int. J.* **19,** 178–188 (2015).

109. Lin, Y.-C. *et al.* Thermodynamics, Kinetics and Structural Evolution of ε-LiVOPO4 over Multiple Lithium Intercalation. *Chem Mater* (2015). doi:10.1021/acs.chemmater.5b04880

110. American Elements. Safety Data Sheet - Lithium Manganese Oxide Nanoparticles. (2015).

111. Cheng, F. *et al.* Porous LiMn2O4 nanorods with durable high-rate capability for rechargeable Li-ion batteries. *Energy Environ. Sci.* **4,** 3668 (2011).

112. Li, W. *et al.* A Sulfur Cathode with Pomegranate-Like Cluster Structure. *Adv. Energy Mater.* **5,** (2015).

113. Xu, R., Lu, J. & Amine, K. Progress in Mechanistic Understanding and Characterization Techniques of Li-S Batteries. *Adv. Energy Mater.* **5,** 1–22 (2015).

114. Cai, K., Song, M.-K., Cairns, E. J. & Zhang, Y. Nanostructured Li_2S-C composites as cathode material for high-energy lithium/sulfur batteries. *Nano Lett.* **12,** 6474–9 (2012).

115. Wu, S., Ge, R., Lu, M., Xu, R. & Zhang, Z. Graphene-based nano-materials for lithium-sulfur battery and sodium-ion battery. *Nano Energy* **15,** 379–405 (2015).

116. Son, Y., Lee, J. S., Son, Y., Jang, J. H. & Cho, J. Recent Advances in Lithium Sulfide Cathode Materials and Their Use in Lithium Sulfur Batteries. *Adv. Energy Mater.* **5,** 1–14 (2015).

117. Manthiram, A., Chung, S.-H. & Zu, C. Lithium–Sulfur Batteries: Progress and Prospects. *Adv. Mater.* **27,** 1980–2006 (2015).

118. American Elements. Safety Data Sheet - Sulfur Nanopowder. (2015).

119. American Polymer Standards Corporation. MSDS Information. Available at: http://www.ampolymer.com/I5-MSDS.html.

120. Globale EHS-Manages. Sicherheitsdatenblatt - Polyaniline. (2012).

121. Nan, C. *et al.* Durable carbon-coated Li2(S) core-shell spheres for high performance lithium/sulfur cells. *J. Am. Chem. Soc.* **136,** 4659–63 (2014).

122. Yang, Y. *et al.* High-Capacity Micrometer-Sized Li2S Particles as Cathode Materials for Advanced Rechargeable Lithium-Ion Batteries. *J. Am. Chem. Soc.* **134,** 15387–15394 (2012).

123. Georgi-Maschler, T., Friedrich, B., Weyhe, R., Heegn, H. & Rutz, M. Development of a recycling process for Li-ion batteries. *J. Power Sources* **207,** 173–182 (2012).

124. Reuter, M. A. *et al. UNEP (2013) Metal Recycling: Opportunities, Limits, Infrastructure, A Report of the Working Group on the Global Metal Flows to the International Resource Panel.* (2013).

125. Gratz, E., Sa, Q., Apelian, D. & Wang, Y. A closed loop process for recycling spent lithium ion batteries. *J. Power Sources* **262,** 255–262 (2014).

126. Xu, J. *et al.* A review of processes and technologies for the recycling of lithium-ion secondary batteries. *J. Power Sources* **177,** 512–527 (2008).

127. Accurec. Personal communication. (2016).

128. Umicore. Personal communication. (2015).

129. Som, C. *et al.* The importance of life cycle concepts for the development of safe nanoproducts. *Toxicology* **269,** 160–169 (2010).

130. Honda. Honda FCV Concept - Official Site. Available at: http://automobiles.honda.com/honda%2Dfcv/. (Accessed: 9th December 2015)

131. Toyota Mirai. Available at: https://ssl.toyota.com/mirai-questionnaire/. (Accessed: 9th December 2015)

132. Scofield, M. E., Liu, H. & Wong, S. S. A concise guide to sustainable PEMFCs: recent advances in improving both oxygen reduction catalysts and proton exchange membranes. *Chem. Soc. Rev.* **44,** 5836–60 (2015).

133. Duan, H. & Xu, C. Nanoporous PtPd Alloy Electrocatalysts with High Activity and Stability toward Oxygen Reduction Reaction. *Electrochim. Acta* **152,** 417–424 (2015).

134. Chen, Z., Higgins, D., Yu, A., Zhang, L. & Zhang, J. A review on non-precious metal electrocatalysts for PEM fuel cells. *Energy Environ. Sci.* **4,** 3167 (2011).

135. Shao, M., Chang, Q., Dodelet, J.-P. & Chenitz, R. Recent Advances in Electrocatalysts for Oxygen Reduction Reaction. *Chem. Rev.* **116,** 3594–3657 (2016).

136. Morozan, A., Jousselme, B. & Palacin, S. Low-platinum and platinum-free catalysts for the oxygen reduction reaction at fuel cell cathodes. *Energy Environ. Sci.* **4,** 1238 (2011).

137. Zhang, W. & Pintauro, P. N. High-Performance Nanofiber Fuel Cell Electrodes. *ChemSusChem* **4,** 1753–1757 (2011).

138. Brodt, M. *et al.* Fabrication, In-Situ Performance, and Durability of Nanofiber Fuel Cell Electrodes. *J. Electrochem. Soc.* **162,** F84–F91 (2014).

139. Alia, S. M. *et al.* Platinum-Coated Nickel Nanowires as Oxygen-Reducing Electrocatalysts. *ACS Catal.* **4,** 1114–1119 (2014).

140. Wang, C., Markovic, N. M. & Stamenkovic, V. R. Advanced Platinum Alloy Electrocatalysts for the Oxygen Reduction Reaction. (2012).

141. Choi, S.-I. *et al.* Synthesis and characterization of 9 nm Pt-Ni octahedra with a record high activity of 3.3 A/mg(Pt) for the oxygen reduction reaction. *Nano Lett.* **13,** 3420–5 (2013).

142. Guo, S. *et al.* FePt and CoPt nanowires as efficient catalysts for the oxygen reduction reaction. *Angew. Chem. Int. Ed. Engl.* **52,** 3465–8 (2013).

143. Tseng, C.-J., Lo, S.-T., Lo, S.-C. & Chu, P. P. Characterization of Pt-Cu binary catalysts for oxygen reduction for fuel cell applications. *Mater. Chem. Phys.* **100,** 385–390 (2006).

144. Liu, J. *et al.* Impact of Cu-Pt nanotubes with a high degree of alloying on electro-catalytic activity toward oxygen reduction reaction. *Electrochim. Acta* **152,** 425–432 (2015).

145. Nuss, P. & Eckelman, M. J. Life cycle assessment of metals: A scientific synthesis. *PLoS One* **9,** 1–12 (2014).

146. Proietti, E. *et al.* Iron-based cathode catalyst with enhanced power density in polymer electrolyte membrane fuel cells. *Nat. Commun.* **2,** 416 (2011).

147. Choi, C. H., Chung, M. W., Jun, Y. J. & Woo, S. I. Doping of chalcogens (sulfur and/or selenium) in nitrogen-doped graphene–CNT self-assembly for enhanced oxygen reduction activity in acid media. *RSC Adv.* **3,** 12417 (2013).

148. Wei, Q. *et al.* Nitrogen-Doped Carbon Nanotube and Graphene Materials for Oxygen Reduction Reactions. *Catalysts* **5,** 1574–1602 (2015).

149. Zhan, Y. *et al.* Iodine/nitrogen co-doped graphene as metal free catalyst for oxygen

reduction reaction. *Carbon N. Y.* **95,** 930–939 (2015).

150. Li, H. *et al.* A review of water flooding issues in the proton exchange membrane fuel cell. *J. Power Sources* **178,** 103–117 (2008).

151. Higgins, D. *et al.* Development and Simulation of Sulfur-doped Graphene Supported Platinum with Exemplary Stability and Activity Towards Oxygen Reduction. *Adv. Funct. Mater.* **24,** 4325–4336 (2014).

152. Shahgaldi, S. & Hamelin, J. Improved carbon nanostructures as a novel catalyst support in the cathode side of PEMFC: a critical review. *Carbon N. Y.* **94,** 705–728 (2015).

153. Sharma, S. & Pollet, B. G. Support materials for PEMFC and DMFC electrocatalysts—A review. *J. Power Sources* **208,** 96–119 (2012).

154. Higgins, D. C., Meza, D. & Chen, Z. Nitrogen-Doped Carbon Nanotubes as Platinum Catalyst Supports for Oxygen Reduction Reaction in Proton Exchange Membrane Fuel Cells. *J. Phys. Chem. C* **114,** 21982–21988 (2010).

155. Yee, R. S. L., Rozendal, R. A., Zhang, K. & Ladewig, B. P. Cost effective cation exchange membranes: A review. *Chem. Eng. Res. Des.* **90,** 950–959 (2012).

156. Hongsirikarn, K., Goodwin, J. G., Greenway, S. & Creager, S. Influence of ammonia on the conductivity of Nafion membranes. *J. Power Sources* **195,** 30–38 (2010).

157. Tripathi, B. P. & Shahi, V. K. Organic–inorganic nanocomposite polymer electrolyte membranes for fuel cell applications. *Prog. Polym. Sci.* **36,** 945–979 (2011).

158. Kraytsberg, A. & Ein-Eli, Y. Review of Advanced Materials for Proton Exchange Membrane Fuel Cells. *Energy & Fuels* **28,** 7303–7330 (2014).

159. Ballengee, J. B., Haugen, G. M., Hamrock, S. J. & Pintauro, P. N. Properties and Fuel Cell Performance of a Nanofiber Composite Membrane with 660 Equivalent Weight Perfluorosulfonic Acid. *J. Electrochem. Soc.* **160,** F429–F435 (2013).

160. Tanaka, M. Development of ion conductive nanofibers for polymer electrolyte fuel cells. *Polym. J.* **48,** 51–58 (2015).

161. Wycisk, R., Pintauro, P. N. & Park, J. W. New developments in proton conducting membranes for fuel cells. *Curr. Opin. Chem. Eng.* **4,** 71–78 (2014).

162. Ballengee, J. B. & Pintauro, P. N. Composite Fuel Cell Membranes from Dual-Nanofiber Electrospun Mats. (2011).

163. Subianto, S. Recent advances in polybenzimidazole/phosphoric acid membranes for high-temperature fuel cells. *Polym. Int.* **63,** 1134–1144 (2014).

164. Ted Pella Inc. *Safety Data Sheet Product - Phosphotungstic Acid*. (2015).

165. Jun, Y., Zarrin, H., Fowler, M. & Chen, Z. Functionalized titania nanotube composite membranes for high temperature proton exchange membrane fuel cells. *Int. J. Hydrogen Energy* **36,** 6073–6081 (2011).

166. Wang, Y., Jin, J., Yang, S., Li, G. & Qiao, J. Highly active and stable platinum catalyst supported on porous carbon nanofibers for improved performance of PEMFC. *Electrochim. Acta* **177,** 181–189 (2015).

167. Chalkovaa, E. *et al.* Composite Proton Conductive Membranes for Elevated Temperature and Reduced Relative Humidity PEMFC. in *ECS Transactions* **25,** 1141–1150 (ECS, 2009).

168. Kalappa, P. & Lee, J.-H. Proton conducting membranes based on sulfonated poly(ether ether ketone)/TiO2 nanocomposites for a direct methanol fuel cell. *Polym. Int.* **56,** 371–375 (2007).

169. Chandan, A. *et al.* High temperature (HT) polymer electrolyte membrane fuel cells (PEMFC) – A review. *J. Power Sources* **231,** 264–278 (2013).

170. Lu, J., Lu, S. & Jiang, S. P. Highly ordered mesoporous Nafion membranes for fuel cells. *Chem. Commun. (Camb).* **47,** 3216–8 (2011).

171. Patel, A. & Dawson, R. Recovery of platinum group metal value via potassium iodide leaching. *Hydrometallurgy* **157,** 219–225 (2015).

172. Columbus Chemical Industries Inc. Safety data sheet - Sodium Cyanide. 1–6 (2014).

173. Airgas. Safety Data Sheet - Chlorine. 1–6 (2015). doi:10.1021/ie50466a600

174. Columbus Chemical Industries Inc. Safety Data Sheet - Aqua Regia. 1–7 (2013).

175. Handley, C., Brandon, N. P. & Van Der Vorst, R. Impact of the European Union vehicle waste directive on end-of-life options for polymer electrolyte fuel cells. *J. Power Sources* **106,** 344–352 (2002).

176. Shiroishi, H. *et al.* Dissolution Rate of Noble Metals for Electrochemical Recycle in Polymer Electrolyte Fuel Cells. *Electrochemistry* 7–12 (2012).

177. Xu, F., Mu, S. & Pan, M. Recycling of membrane electrode assembly of PEMFC by acid processing. *Int. J. Hydrogen Energy* **35,** 2976–2979 (2010).

178. Peng, B., Cheng, F., Tao, Z. & Chen, J. Lithium transport at silicon thin film: Barrier for high-rate capability anode. *J. Chem. Phys.* **133,** 1–6 (2010).

179. Park, T.-H. *et al.* Enhancing the rate performance of graphite anodes through addition of natural graphite/carbon nanofibers in lithium-ion batteries. *Electrochim. Acta* **93,** 236–240 (2013).

180. Gavankar, S., Suh, S. & Keller, A. A. The Role of Scale and Technology Maturity in Life

Cycle Assessment of Emerging Technologies: A Case Study on Carbon Nanotubes. *J. Ind. Ecol.* **19,** 51–60 (2015).

181. American Elements. Safety Data Sheet - Silicon Oxide Hollow Nanoshperes. 6–13 (2015).

182. Cui, L.-F., Ruffo, R., Chan, C. K., Peng, H. & Cui, Y. Crystalline-Amorphous Core−Shell Silicon Nanowires for High Capacity and High Current Battery Electrodes. *Nano Lett.* **9,** 491–495 (2009).

183. Luo, Z. *et al.* High performance silicon carbon composite anode materials for lithium ion batteries. *J. Power Sources* **189,** 16–21 (2009).

184. Park, M. H. *et al.* Silicon nanotube battery anodes. *Nano Lett.* **9,** 3844–3847 (2009).

185. Li, N. A High-Rate, High-Capacity, Nanostructured Tin Oxide Electrode. *Electrochem. Solid-State Lett.* **3,** 316 (1999).

186. Yin, X. *et al.* Synthesis of mesoporous SnO2 spheres via self-assembly and superior lithium storage properties. *Electrochim. Acta* **56,** 2358–2363 (2011).

187. Kennedy, T. *et al.* High-performance germanium nanowire-based lithium-ion battery anodes extending over 1000 cycles through in situ formation of a continuous porous network. *Nano Lett.* **14,** 716–23 (2014).

188. American Elements. Safety Data Sheet - Germanium Oxide Nanopowder. (2015).

189. Yuan, F.-W., Yang, H.-J. & Tuan, H.-Y. Alkanethiol-Passivated Ge Nanowires as High-Performance Anode Materials for Lithium-Ion Batteries: The Role of Chemical Surface Functionalization. *ACS Nano* **6,** 9932–9942 (2012).

190. Chockla, A. M., Klavetter, K. C., Mullins, C. B. & Korgel, B. A. Solution-Grown Germanium Nanowire Anodes for Lithium-Ion Batteries. (2012).

191. Koo, B. *et al.* Hollow Iron Oxide Nanoparticles for Application in Lithium Ion Batteries. (2012).

192. Meng, Q. *et al.* Facile fabrication of mesoporous N-doped Fe3O4@C nanospheres as superior anodes for Li-ion batteries. *RSC Adv.* **4,** 713 (2014).

193. Li, H., Balaya, P. & Maier, J. Li-Storage via Heterogeneous Reaction in Selected Binary Metal Fluorides and Oxides. *J. Electrochem. Soc.* **151,** A1878 (2004).

194. Courtel, F. M., Duncan, H. & Abu-lebdeh, Y. in *Nanotechnology for Lithium-Ion Batteries* 85–116 (2013). doi:10.1007/978-1-4614-4605-7_5

195. He, C. *et al.* Carbon-Encapsulated Fe 3 O 4 Nanoparticles as a High-Rate Lithium Ion Battery Anode Material. *ACS Nano* 4459–4469 (2013). doi:Doi 10.1021/Nn401059h

196. Chen, C. H. *et al.* An understanding of anomalous capacity of nano-sized CoO anode materials for advanced Li-ion battery. *Electrochem. commun.* **12,** 496–498 (2010).

197. Wu, Z. *et al.* Graphene Anchored with Co 3 O 4 Nanoparticles as Anode of Lithium Ion Capacity and Cyclic Performance. *ACS Nano* **4,** 3187–3194 (2010).

198. Chen, L. B., Lu, N., Xu, C. M., Yu, H. C. & Wang, T. H. Electrochemical performance of polycrystalline CuO nanowires as anode material for Li ion batteries. *Electrochim. Acta* **54,** 4198–4201 (2009).

199. Sigma Aldrich. Safety data sheet - Ruthenium (IV) oxide. 1–7 (2014).

200. American Elements. Safety Data Sheet - Nickel Oxide Nanopowder. (2015).

201. Wang, X. *et al.* Nanostructured NiO electrode for high rate Li-ion batteries. *J. Mater. Chem.* **21,** 3571 (2011).

202. American Elements. Safety Data Sheet - Manganese Oxide Nanopowder. 1–9 (2015).

203. Gao, J., Lowe, M. a & Abru, D. Spongelike Nanosized Mn 3 O 4 as a High-Capacity Anode Material for Rechargeable Lithium Batteries. *Chem. Mater.* 3223–3227 (2011). doi:10.1021/cm201039w

204. Kim, T.-H. *et al.* The Current Move of Lithium Ion Batteries Towards the Next Phase. *Adv. Energy Mater.* **2,** 860–872 (2012).

205. Mulder, G. *et al.* Comparison of commercial battery cells in relation to material properties. *Electrochim. Acta* **87,** 473–488 (2013).

206. Wu, Y., Cao, C., Zhu, Y., Li, J. & Wang, L. Cube-shaped hierarchical LiNi $_{1/3}$ Co $_{1/3}$ Mn $_{1/3}$ O $_{2}$ with enhanced growth of nanocrystal planes as high-performance cathode materials for lithium-ion batteries. *J. Mater. Chem. A* **3,** 15523–15528 (2015).

207. Li, J., Cao, C., Xu, X., Zhu, Y. & Yao, R. LiNi1/3Co1/3Mn1/3O2 hollow nano-micro hierarchical microspheres with enhanced performances as cathodes for lithium-ion batteries. *J. Mater. Chem. A* **1,** 11848 (2013).

208. Fergus, J. W. Recent developments in cathode materials for lithium ion batteries. *J. Power Sources* **195,** 939–954 (2010).

209. Huang, Z.-D. *et al.* Microscopically porous, interconnected single crystal LiNi1/3Co1/3Mn1/3O2 cathode material for Lithium ion batteries. *J. Mater. Chem.* **21,** 10777 (2011).

210. Hanisch, C. *et al.* Recycling of lithium-ion batteries: a novel method to separate coating and foil of electrodes. *J. Clean. Prod.* **108,** 301–311 (2015).

211. Thackeray, M. M., Wolverton, C. & Isaacs, E. D. Electrical energy storage for transportation—approaching the limits of, and going beyond, lithium-ion batteries.

Energy Environ. Sci. **5,** 7854 (2012).

212. Anseán, D. *et al.* Fast charging technique for high power lithium iron phosphate batteries: A cycle life analysis. *J. Power Sources* **239,** 9–15 (2013).

213. Saravanan, K., Lee, H. S., Kuezma, M., Vittal, J. J. & Balaya, P. Hollow α-LiVOPO4 sphere cathodes for high energy Li-ion battery application. *J. Mater. Chem.* **21,** 10042 (2011).

214. Quackenbush, N. F. *et al.* Interfacial Effects in ε-LixVOPO4 and Evolution of the Electronic Structure. *Chem. Mater.* **27,** 8211–8219 (2015).

215. Lee, H.-W. *et al.* Ultrathin Spinel $LiMn_2O_4$ Nanowires as High Power Cathode Materials for Li-Ion Batteries. *Nano Lett.* **10,** 3852–3856 (2010).

216. Ahn, W. *et al.* Sulfur Nanogranular Film-Coated Three-Dimensional Graphene Sponge-Based High Power Lithium Sulfur Battery. *ACS Appl. Mater. Interfaces* acsami.5b10267 (2016). doi:10.1021/acsami.5b10267

217. Chen, R. *et al.* Graphene-based three-dimensional hierarchical sandwich-type architecture for high-performance Li/S batteries. *Nano Lett.* **13,** 4642–4649 (2013).

218. Li, W. *et al.* High-performance hollow sulfur nanostructured battery cathode through a scalable, room temperature, one-step, bottom-up approach. *Proc. Natl. Acad. Sci. U. S. A.* **110,** 7148–53 (2013).

219. Papandrea, B. *et al.* Three-dimensional graphene framework with ultra-high sulfur content for a robust lithium–sulfur battery. *Nano Res.* **9,** 240–248 (2016).

220. Peng, H.-J. *et al.* Nanoarchitectured Graphene/CNT@Porous Carbon with Extraordinary Electrical Conductivity and Interconnected Micro/Mesopores for Lithium-Sulfur Batteries. *Adv. Funct. Mater.* **24,** 2772–2781 (2014).

221. Song, M., Zhang, Y. & Cairns, E. J. A Long-Life, High-Rate Lithium/Sulfur Cell: A Multifaceted Approach to Enhancing Cell Performance. (2013). doi:10.1021/nl402793z

222. Su, Y. S. & Manthiram, A. Lithium-sulphur batteries with a microporous carbon paper as a bifunctional interlayer. *Nat Commun* **3,** 1166 (2012).

223. Wang, C. *et al.* Macroporous free-standing nano-sulfur/reduced graphene oxide paper as stable cathode for lithium-sulfur battery. *Nano Energy* **11,** 678–686 (2015).

224. Xiao, L. *et al.* A soft approach to encapsulate sulfur: Polyaniline nanotubes for lithium-sulfur batteries with long cycle life. *Adv. Mater.* **24,** 1176–81 (2012).

225. Zhao, M.-Q. *et al.* Unstacked double-layer templated graphene for high-rate lithium-sulphur batteries. *Nat. Commun.* **5,** 3410 (2014).

226. Zheng, S. *et al.* In Situ Formed Lithium Sulfide / Microporous Carbon Cathodes for

Lithium-Ion Batteries. *ACS Nano* **7,** 10995–11003 (2013).

227. Zheng, G. *et al.* Amphiphilic Surface Modification of Hollow Carbon Nanofibers for Improved Cycle Life of Lithium Sulfur Batteries. 8–13 (2013). doi:dx.doi.org/10.1021/nl304795g

228. Zhou, W., Yu, Y., Chen, H. & Disalvo, F. J. Yolk − Shell Structure of Polyaniline-Coated Sulfur for Lithium − Sulfur Batteries. (2013).

229. Zhou, G. *et al.* A graphene foam electrode with high sulfur loading for flexible and high energy Li-S batteries. *Nano Energy* **11,** 356–365 (2015).

230. Sigma Aldrich. Safety data sheet - Polyacrylonitrile. 1–6 (2014).

231. Science Lab. *Material Safety Data Sheet - Polyvinylpyrrolidone*. (2013).

232. Zhang, K., Wang, L., Hu, Z., Cheng, F. & Chen, J. Ultrasmall Li_2S Nanoparticles Anchored in Graphene Nanosheets for High-Energy Lithium-Ion Batteries. *Sci. Rep.* **4,** 6467 (2014).

233. Yang, Z. *et al.* In situ synthesis of lithium sulfide-carbon composites as cathode materials for rechargeable lithium batteries. *J. Mater. Chem. A Mater. Energy Sustain.* **1,** 1433–1440 (2013).

234. Sigma Aldrich. *Safety data sheet - Platinum, nanoparticle dispersion*. 1–6 (2015).

235. Li, W. *et al.* Preparation and Characterization of Multiwalled Carbon Nanotube-Supported Platinum for Cathode Catalysts of Direct Methanol Fuel Cells. *J. Phys. Chem. B* **107,** 6292–6299 (2003).

236. Hagelüken, C. Recycling the Platinum Group Metals: A European Perspective. *Platin. Met. Rev.* **56,** 29–35 (2012).

237. Andersen, S. M. *et al.* Durability of carbon nanofiber (CNF) & carbon nanotube (CNT) as catalyst support for Proton Exchange Membrane Fuel Cells. *Solid State Ionics* **231,** 94–101 (2013).

238. Fu, G. *et al.* Polyallylamine-directed green synthesis of platinum nanocubes. Shape and electronic effect codependent enhanced electrocatalytic activity. *Phys. Chem. Chem. Phys.* **15,** 3793–802 (2013).

239. Sun, S. *et al.* A Highly Durable Platinum Nanocatalyst for Proton Exchange Membrane Fuel Cells: Multiarmed Starlike Nanowire Single Crystal. *Angew. Chemie Int. Ed.* **50,** 422–426 (2011).

240. Li, B. *et al.* The durability of carbon supported Pt nanowire as novel cathode catalyst for a 1.5kW PEMFC stack. *Appl. Catal. B Environ.* **162,** 133–140 (2015).

241. Li, B. *et al.* Carbon-supported Pt nanowire as novel cathode catalysts for proton

exchange membrane fuel cells. *J. Power Sources* **262,** 488–493 (2014).

242. Zhang, L. *et al.* Highly stable PtP alloy nanotube arrays as a catalyst for the oxygen reduction reaction in acidic medium. *Chem. Sci.* **6,** 3211–3216 (2015).

243. Nguyen, T.-T. *et al.* Synthesis of Ti0.7Mo0.3O2 supported-Pt nanodendrites and their catalytic activity and stability for oxygen reduction reaction. *Appl. Catal. B Environ.* **154-155,** 183–189 (2014).

244. Daimon, H. *et al.* Change in ORR Activity of PtPd/C Alloy and Pt/Pd/C Core-Shell Catalysts with Accelerated Durability Test. *Meet. Abstr.* **MA2014-02 ,** 1063 (2014).

245. Okuno, K. *et al.* Enhancement of ORR Activity of PtPd/C Alloy Catalyst with Accelerated Durability Test and Chemical De-Alloying. *Meet. Abstr.* **MA2015-02,** 1405 (2015).

246. Holade, Y., Sahin, N., Servat, K., Napporn, T. & Kokoh, K. Recent Advances in Carbon Supported Metal Nanoparticles Preparation for Oxygen Reduction Reaction in Low Temperature Fuel Cells. *Catalysts* **5,** 310–348 (2015).

247. Chen, C. *et al.* Highly crystalline multimetallic nanoframes with three-dimensional electrocatalytic surfaces. *Science* **343,** 1339–43 (2014).

248. Cui, C. *et al.* Octahedral PtNi Nanoparticle Catalysts: Exceptional Oxygen Reduction Activity by Tuning the Alloy Particle Surface Composition. *Nano Lett.* **12,** 5885–5889 (2012).

249. Carpenter, M. K., Moylan, T. E., Kukreja, R. S., Atwan, M. H. & Tessema, M. M. Solvothermal synthesis of platinum alloy nanoparticles for oxygen reduction electrocatalysis. *J. Am. Chem. Soc.* **134,** 8535–42 (2012).

250. Zhang, C., Hwang, S. Y., Trout, A. & Peng, Z. Solid-state chemistry-enabled scalable production of octahedral Pt-Ni alloy electrocatalyst for oxygen reduction reaction. *J. Am. Chem. Soc.* **136,** 7805–8 (2014).

251. Xu, X. *et al.* Synthesis of Pt–Ni Alloy Nanocrystals with High-Index Facets and Enhanced Electrocatalytic Properties. *Angew. Chemie Int. Ed.* **53,** 12522–12527 (2014).

252. Koenigsmann, C., Sutter, E., Chiesa, T. A., Adzic, R. R. & Wong, S. S. Highly enhanced electrocatalytic oxygen reduction performance observed in bimetallic palladium-based nanowires prepared under ambient, surfactantless conditions. *Nano Lett.* **12,** 2013–20 (2012).

253. Wang, G. *et al.* Pt skin on AuCu intermetallic substrate: a strategy to maximize Pt utilization for fuel cells. *J. Am. Chem. Soc.* **136,** 9643–9 (2014).

254. Wang, G. *et al.* AuCu intermetallic nanoparticles: surfactant-free synthesis and novel electrochemistry. *J. Mater. Chem.* **22,** 15769 (2012).

255. Strem Chemicals Inc. *Safety Data Sheet - copper nanoparticles*. (2016).

256. Sievers, G. *et al.* Mesoporous Pt–Co oxygen reduction reaction (ORR) catalysts for low temperature proton exchange membrane fuel cell synthesized by alternating sputtering. *J. Power Sources* **268,** 255–260 (2014).

257. Wang, D.-Y. *et al.* FePt nanodendrites with high-index facets as active electrocatalysts for oxygen reduction reaction. *Nano Energy* **11,** 631–639 (2015).

258. Dai, Y. *et al.* Efficient and Superiorly Durable Pt-Lean Electrocatalysts of Pt−W Alloys for the Oxygen Reduction Reaction. *J. Phys. Chem. C* **115,** 2162–2168 (2011).

259. American Elements. Safety Data Sheet - Palladium Nanoparticles. 1–6 (2015).

260. Xiao, L., Zhuang, L., Liu, Y., Lu, J. & Abruña, H. D. Activating Pd by morphology tailoring for oxygen reduction. *J. Am. Chem. Soc.* **131,** 602–8 (2009).

261. Ted Pella Inc. Material Safety Data Sheet - Colloidal Gold. (2012).

262. Hu, Y. *et al.* Hollow Spheres of Iron Carbide Nanoparticles Encased in Graphitic Layers as Oxygen Reduction Catalysts. *Angew. Chemie Int. Ed.* **53,** 3675–3679 (2014).

263. American Elements. Safety Data Sheet - Iron Carbide. 1–8 (2015).

264. Seo, J., Cha, D., Takanabe, K., Kubota, J. & Domen, K. Electrodeposited Ultrafine NbO x , ZrO x , and TaO x Nanoparticles on Carbon Black Supports for Oxygen Reduction Electrocatalysts in Acidic Media. *ACS Catal.* **3,** 2181–2189 (2013).

265. American Elements. *Safety Data Sheet - Niobium Oxide Nanopowder*. (2012).

266. Kim, J. Y., Oh, T.-K., Shin, Y., Bonnett, J. & Weil, K. S. A novel non-platinum group electrocatalyst for PEM fuel cell application. *Int. J. Hydrogen Energy* **36,** 4557–4564 (2011).

267. American Elements. Safety Data Sheet - Tantalum Oxide Nanopowder. (2015).

268. American Elements. *Safety Data Sheet - Zirconium Oxide Nanopowder*. (2015).

269. Seo, J. *et al.* Highly Dispersed TaO x Nanoparticles Prepared by Electrodeposition as Oxygen Reduction Electrocatalysts for Polymer Electrolyte Fuel Cells. *J. Phys. Chem. C* **117,** 11635–11646 (2013).

270. Wang, H., Liang, Y., Li, Y. & Dai, H. Co(1-x)S-graphene hybrid: a high-performance metal chalcogenide electrocatalyst for oxygen reduction. *Angew. Chem. Int. Ed. Engl.* **50,** 10969–72 (2011).

271. Cao, B. *et al.* Cobalt Molybdenum Oxynitrides: Synthesis, Structural Characterization, and Catalytic Activity for the Oxygen Reduction Reaction. *Angew. Chemie* **125,** 10953–10957 (2013).

272. Ding, W. *et al.* Space-confinement-induced synthesis of pyridinic- and pyrrolic-nitrogen-doped graphene for the catalysis of oxygen reduction. *Angew. Chem. Int. Ed. Engl.* **52,** 11755–9 (2013).

273. Gong, K., Du, F., Xia, Z., Durstock, M. & Dai, L. Nitrogen-doped carbon nanotube arrays with high electrocatalytic activity for oxygen reduction. *Science* **323,** 760–4 (2009).

274. Shui, J., Wang, M., Du, F. & Dai, L. N-doped carbon nanomaterials are durable catalysts for oxygen reduction reaction in acidic fuel cells. *Sci. Adv.* **1,** e1400129–e1400129 (2015).

275. Peera, S. G. *et al.* Nitrogen and fluorine co-doped graphite nanofibers as high durable oxygen reduction catalyst in acidic media for polymer electrolyte fuel cells. *Carbon N. Y.* **93,** 130–142 (2015).

276. Choi, C. H., Park, S. H. & Woo, S. I. Phosphorus–nitrogen dual doped carbon as an effective catalyst for oxygen reduction reaction in acidic media: effects of the amount of P-doping on the physical and electrochemical properties of carbon. *J. Mater. Chem.* **22,** 12107 (2012).

277. Choi, C. H., Chung, M. W., Kwon, H. C., Park, S. H. & Woo, S. I. B, N- and P, N-doped graphene as highly active catalysts for oxygen reduction reactions in acidic media. *J. Mater. Chem. A* **1,** 3694 (2013).

278. Choi, C. H., Chung, M. W., Park, S. H. & Woo, S. I. Additional doping of phosphorus and/or sulfur into nitrogen-doped carbon for efficient oxygen reduction reaction in acidic media. *Phys. Chem. Chem. Phys.* **15,** 1802–5 (2013).

279. Choi, C. H., Park, S. H. & Woo, S. I. Binary and Ternary Doping of Nitrogen, Boron, and Phosphorus into Carbon for Enhancing Electrochemical Oxygen Reduction Activity. *ACS Nano* **6,** 7084–7091 (2012).

280. Sigma Aldrich. *Safety data sheet - carbon, mesoporous*. (2015).

281. Kou, R. *et al.* Enhanced activity and stability of Pt catalysts on functionalized graphene sheets for electrocatalytic oxygen reduction. *Electrochem. commun.* **11,** 954–957 (2009).

282. Yun, Y. S., Kim, D., Tak, Y. & Jin, H.-J. Porous graphene/carbon nanotube composite cathode for proton exchange membrane fuel cell. *Synth. Met.* **161,** 2460–2465 (2011).

283. Su, F. *et al.* Pt Nanoparticles Supported on Nitrogen-Doped Porous Carbon Nanospheres as an Electrocatalyst for Fuel Cells †. *Chem. Mater.* **22,** 832–839 (2010).

284. Chen, Z., Deng, W., Wang, X. & Yan, Y. Durability and Activity Study of Single-Walled, Double-Walled and Multi-Walled Carbon Nanotubes Supported Pt Catalyst for PEMFCs. in *ECS Transactions* **11,** 1289–1299 (ECS, 2007).

285. Lee, T. K., Jung, J. H., Kim, J. B. & Hur, S. H. Improved durability of Pt/CNT catalysts by the low temperature self-catalyzed reduction for the PEM fuel cells. *Int. J. Hydrogen Energy* **37,** 17992–18000 (2012).

286. Seger, B. & Kamat, P. V. Electrocatalytically Active Graphene-Platinum Nanocomposites. Role of 2-D Carbon Support in PEM Fuel Cells. *J. Phys. Chem. C* **113,** 7990–7995 (2009).

287. Long, D. *et al.* Partially unzipped carbon nanotubes as a superior catalyst support for PEM fuel cells. *Chem. Commun. (Camb).* **47,** 9429–31 (2011).

288. Jafri, R. I., Arockiados, T., Rajalakshmi, N. & Ramaprabhu, S. Nanostructured Pt Dispersed on Graphene-Multiwalled Carbon Nanotube Hybrid Nanomaterials as Electrocatalyst for PEMFC. *J. Electrochem. Soc.* **157,** B874 (2010).

289. Du, H.-Y. *et al.* Graphene nanosheet–CNT hybrid nanostructure electrode for a proton exchange membrane fuel cell. *Int. J. Hydrogen Energy* **37,** 18989–18995 (2012).

290. Aravind, S. S. J. & Ramaprabhu, S. Pt nanoparticle-dispersed graphene-wrapped MWNT composites as oxygen reduction reaction electrocatalyst in proton exchange membrane fuel cell. *ACS Appl. Mater. Interfaces* **4,** 3805–10 (2012).

291. Park, S. *et al.* Design of graphene sheets-supported Pt catalyst layer in PEM fuel cells. *Electrochem. commun.* **13,** 258–261 (2011).

292. Li, W., Waje, M., Chen, Z., Larsen, P. & Yan, Y. Platinum nanopaticles supported on stacked-cup carbon nanofibers as electrocatalysts for proton exchange membrane fuel cell. *Carbon N. Y.* **48,** 995–1003 (2010).

293. Sigma Aldrich. Material safety data sheet - Nafion perflourinated ion-exchange. (2006).

294. Avcioglu, G. S., Ficicilar, B., Bayrakceken, A. & Eroglu, I. High performance PEM fuel cell catalyst layers with hydrophobic channels. *Int. J. Hydrogen Energy* **40,** 7720–7731 (2015).

295. Shao, Y. *et al.* Highly durable graphene nanoplatelets supported Pt nanocatalysts for oxygen reduction. *J. Power Sources* **195,** 4600–4605 (2010).

296. Nam, K.-W. *et al.* Perfluorosulfonic acid-functionalized Pt/graphene as a high-performance oxygen reduction reaction catalyst for proton exchange membrane fuel cells. *J. Solid State Electrochem.* **17,** 767–774 (2012).

297. Zhu, J., He, G., Liang, L., Wan, Q. & Shen, P. K. Direct anchoring of platinum nanoparticles on nitrogen and phosphorus-dual-doped carbon nanotube arrays for oxygen reduction reaction. *Electrochim. Acta* **158,** 374–382 (2015).

298. Liu, Z. *et al.* Phosphorus-doped carbon nanotubes supported low Pt loading catalyst

for the oxygen reduction reaction in acidic fuel cells. *J. Power Sources* **268,** 171–175 (2014).

299. Liu, Z. *et al. Novel phosphorus-doped multiwalled nanotubes with high electrocatalytic activity for O2 reduction in alkaline medium*. *Catalysis Communications* **16,** (2011).

300. American Elements. Safety Data Sheet - Titanium Oxide Nanopowder. (2015).

301. Abdullah, N. & Kamarudin, S. K. Titanium dioxide in fuel cell technology: An overview. *J. Power Sources* **278,** 109–118 (2015).

302. Akalework, N. G. *et al.* Ultrathin TiO2-coated MWCNTs with excellent conductivity and SMSI nature as Pt catalyst support for oxygen reduction reaction in PEMFCs. *J. Mater. Chem.* **22,** 20977 (2012).

303. Du, C., Chen, M., Cao, X., Yin, G. & Shi, P. A novel CNT@SnO2 core–sheath nanocomposite as a stabilizing support for catalysts of proton exchange membrane fuel cells. *Electrochem. commun.* **11,** 496–498 (2009).

304. Graedel, T. E. *et al.* What Do We Know About Metal Recycling Rates? *J. Ind. Ecol.* **15,** 355–366 (2011).

305. Sambandam, S. *et al.* Platinum-carbon black-titanium dioxide nanocomposite electrocatalysts for fuel cell applications. *J. Chem. Sci.* **121,** 655–664 (2009).

306. Huang, S.-Y., Ganesan, P. & Popov, B. N. Titania supported platinum catalyst with high electrocatalytic activity and stability for polymer electrolyte membrane fuel cell. *Appl. Catal. B Environ.* **102,** 71–77 (2011).

307. Bauer, A. *et al.* Pt nanoparticles deposited on TiO2 based nanofibers: Electrochemical stability and oxygen reduction activity. *J. Power Sources* **195,** 3105–3110 (2010).

308. Lo, C.-P., Wang, G., Kumar, A. & Ramani, V. TiO2–RuO2 electrocatalyst supports exhibit exceptional electrochemical stability. *Appl. Catal. B Environ.* **140-141,** 133–140 (2013).

309. Sun, S., Zhang, G., Sun, X., Cai, M. & Ruthkosky, M. Highly stable and active Pt/Nb-TiO2 carbon-free electrocatalyst for proton exchange membrane fuel cells. *J. Nanotechnol.* **2012,** 13–15 (2012).

Acknowledgements

The authors are very thankful to Dong Un Lee and Hadis Zarrin at the University of Waterloo for internal review and helpful discussions. We also express our grateful thanks to Colton Bangs, Dirk Rickert, Maarten Quix, and Charles Stuyck at Umicore and Reiner Weyhe and Qiaoyan Pan at Accurec for helpful communication on recycling of PEMFCs (Umicore) and LIBs (Umicore and Accurec). We also thank Barbara Reck at Yale University for helpful communication. The authors remain solely responsible for the content of this article.

Additional information

Supplementary information accompanies this paper at www.nature.com/naturenanotechnology. Reprints and permission information is available online at http://npg.nature.com/reprintsandpermissions/. Correspondence and requests for materials should be addressed to LE.

Competing financial interests

The authors declare no competing financial interests.

Figures

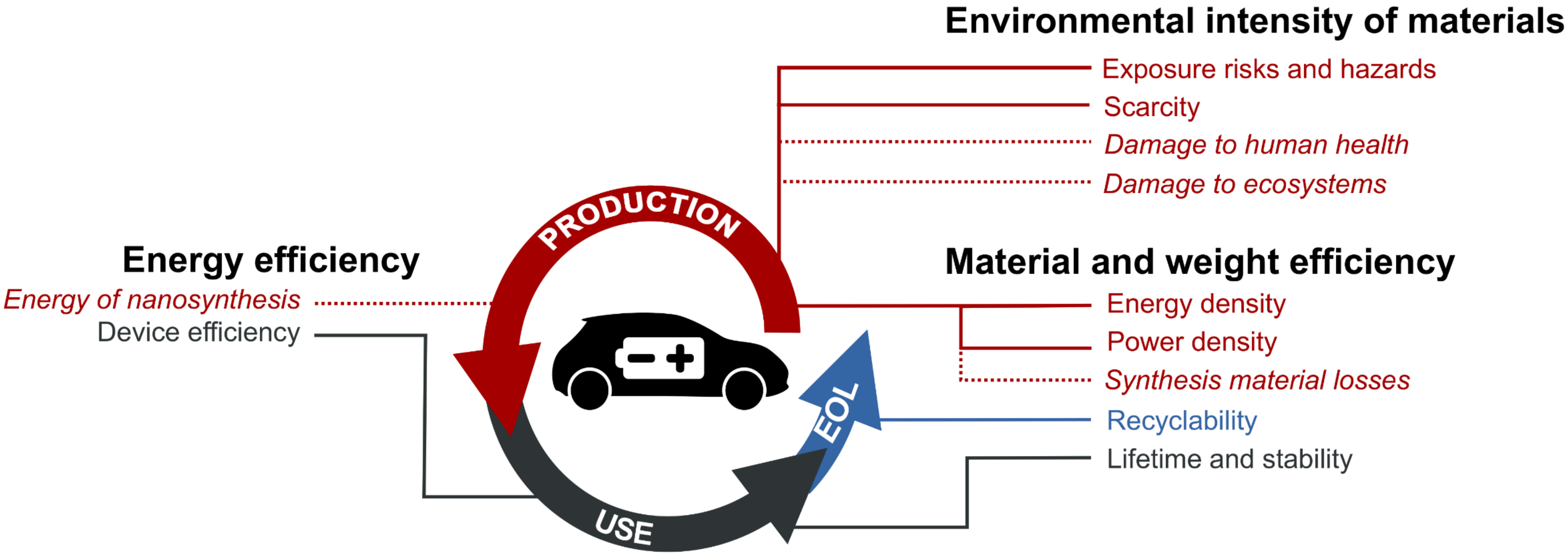

Figure 1 Early lifecycle environmental screening of LIB and PEMFC for electric vehicles. Solid lines denote intrinsic aspects of the material itself. Dotted lines and italic font denote properties that are attributes of the value chain aspects, or embodied activities related to the material's production. Red lines denote production aspects, dark grey lines use phase aspects, and blue lines end-of-life aspects. Abbreviation: EOL – end-of-life.

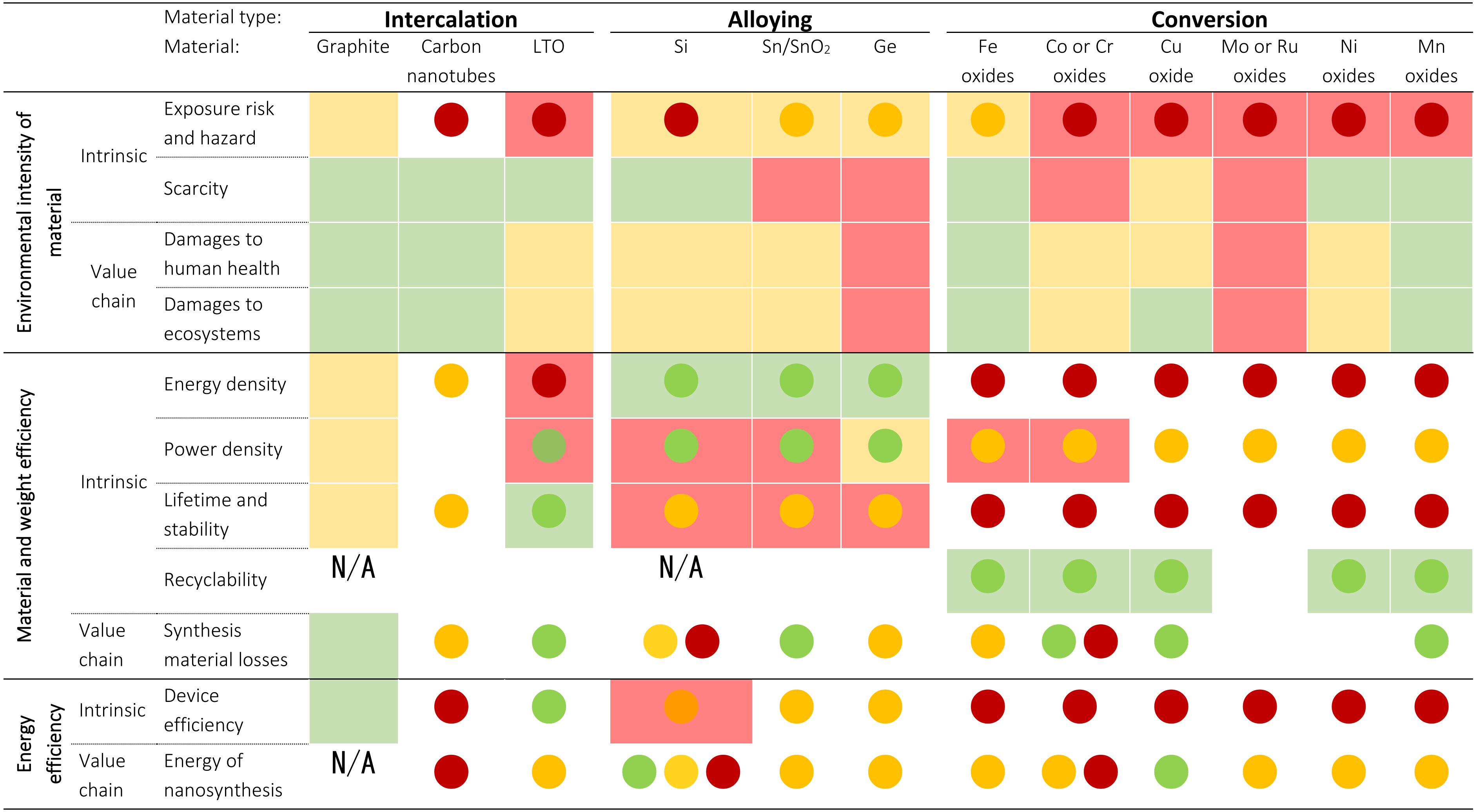

		Material type:	Intercalation			Alloying			Conversion					
		Material:	Graphite	Carbon nanotubes	LTO	Si	Sn/SnO_2	Ge	Fe oxides	Co or Cr oxides	Cu oxide	Mo or Ru oxides	Ni oxides	Mn oxides
Environmental intensity of material	Intrinsic	Exposure risk and hazard	🟨	🔴	🟥 🔴	🟨 🔴	🟨 🟡	🟨 🟡	🟨 🟡	🟥 🔴	🟥 🔴	🟥 🔴	🟥 🔴	🟥 🔴
		Scarcity	🟩	🟩	🟩	🟩	🟥	🟥	🟩	🟥	🟨	🟥	🟩	🟩
	Value chain	Damages to human health	🟩	🟩	🟨	🟨	🟨	🟥	🟩	🟨	🟨	🟥	🟨	🟩
		Damages to ecosystems	🟩	🟩	🟨	🟨	🟨	🟥	🟩	🟨	🟩	🟥	🟨	🟩
Material and weight efficiency	Intrinsic	Energy density	🟨	🟡	🟥 🔴	🟩 🟢	🟩 🟢	🟩 🟢	🔴	🔴	🔴	🔴	🔴	🔴
		Power density	🟨		🟥 🟢	🟥 🟢	🟥 🟢	🟨 🟢	🟥 🟡	🟥 🟡	🟡	🟡	🟡	🟡
		Lifetime and stability	🟨	🟡	🟩 🟢	🟥 🟡	🟥 🟡	🟥 🟡	🔴	🔴	🔴	🔴	🔴	🔴
		Recyclability	N/A			N/A			🟩 🟢	🟩 🟢	🟩 🟢		🟩 🟢	🟩 🟢
	Value chain	Synthesis material losses	🟩	🟡	🟢	🟡 🔴	🟢	🟡	🟡	🟢 🔴	🟢			🟢
Energy efficiency	Intrinsic	Device efficiency	🟩	🔴	🟢	🟥 🟠	🟡	🟡	🔴	🔴	🔴	🔴	🔴	🔴
	Value chain	Energy of nanosynthesis	N/A	🔴	🟡	🟢 🟡 🔴	🟡	🟡	🟡	🟡 🔴	🟢	🟡	🟡	🟡

Figure 2 Anode materials for lithium ion batteries. Nanoarchitectured materials are given by a circle. Background colours reflect characteristics of bulk materials. Green denotes relative strength, red relative weakness, yellow intermediate characteristics, and white no data. Absence of circle indicates no data for nanomaterial. The grey background denotes the 'baseline' material. Abbreviations: LTO – lithium titanium oxide, Si – silicon, Sn – tin, SnO_2- tin oxide, Ge – germanium, Fe – iron, Co – cobalt, Cr – chromium, Cu – copper, Mo – molybdenum, Ru – ruthenium, Ni – nickel, and Mn – manganese. Data from graphite from references [33,47,50–52,54,57,66,178,179]; data from carbon nanotubes from references [12,33,52,56,60,61,180]; data from LTO from references [13,33,34,47,50–52,66–69,71]; data from Si from references [23,33,47,50,51,57,60,66,67,73,75–79,91,181–184]; data from Sn/SnO_2 from references [34,47,50,51,57,66,80,81,185,186]; data from Ge from references [34,47,50,51,57,66,81,187–190]; data from Fe oxides from references [34,50,51,66,68,85,86,91,97,191–195]; data from Co and Cr oxides from references [50,51,66,68,86–88,97,196,197]; data from Cu oxides from references [47,50,51,57,66,68,86,97,198]; data from Mo and Ru oxides from references [47,50,51,66,68,86,89,199]; data from Ni oxides from references [50,51,66,68,86,200,201]; data from Mn oxides from references [47,50,51,66,68,86,202,203]. See the Supplementary citation data for reference details.

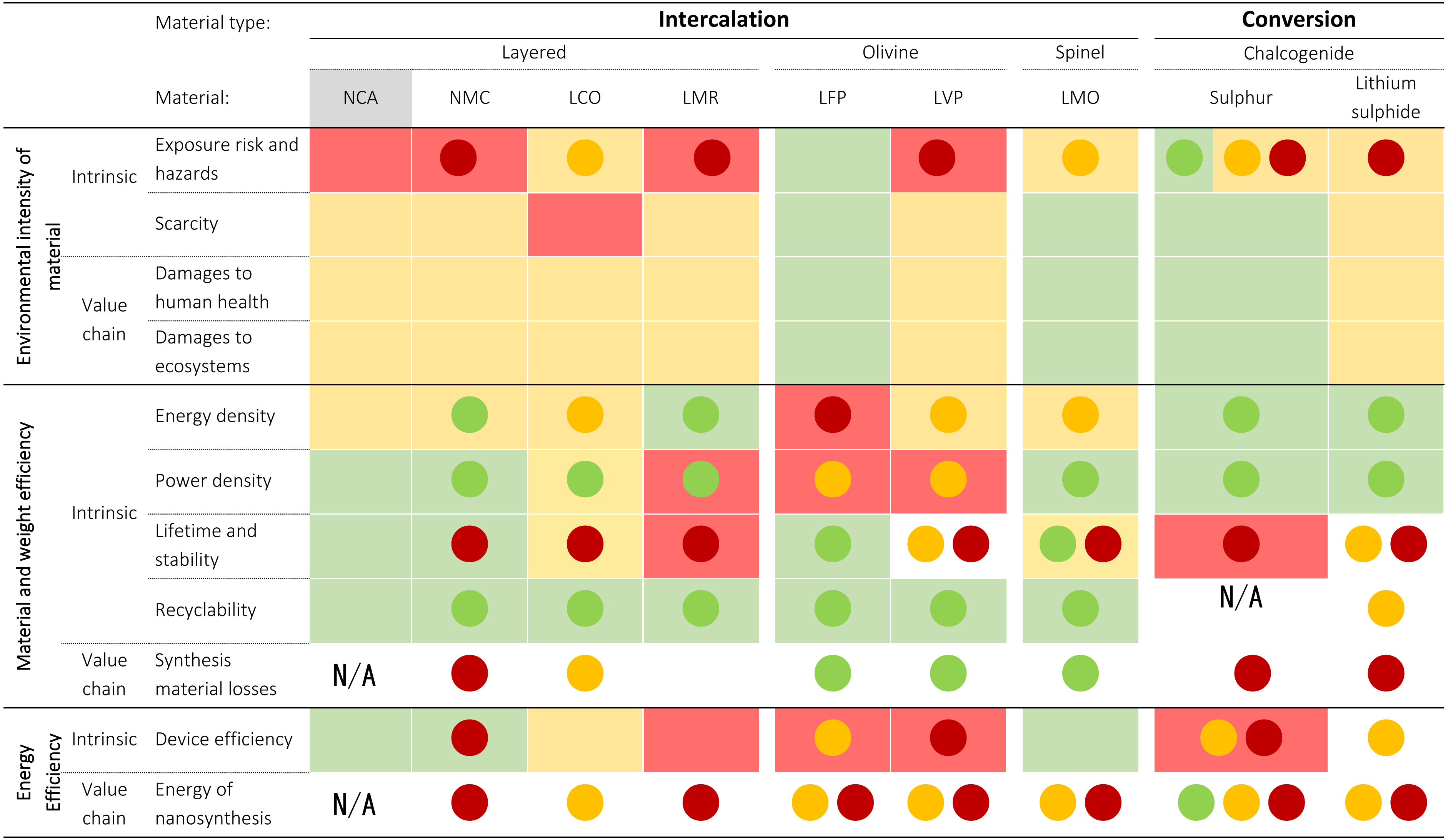

		Material type:	Intercalation							Conversion	
			Layered				Olivine		Spinel	Chalcogenide	
		Material:	NCA	NMC	LCO	LMR	LFP	LVP	LMO	Sulphur	Lithium sulphide
Environmental intensity of material	Intrinsic	Exposure risk and hazards	🟥	🟥 🔴	🟨 🟡	🟥 🔴	🟩	🟥 🔴	🟨 🟡	🟩 🟢 🟨 🟡 🔴	🟨 🔴
		Scarcity	🟨	🟨	🟥	🟨	🟩	🟨	🟩	🟩	🟨
	Value chain	Damages to human health	🟨	🟨	🟨	🟨	🟩	🟨	🟩	🟩	🟨
		Damages to ecosystems	🟨	🟨	🟨	🟨	🟩	🟨	🟩	🟩	🟨
Material and weight efficiency	Intrinsic	Energy density	🟨	🟨 🟢	🟨 🟡	🟩 🟢	🟥 🔴	🟨 🟡	🟨 🟡	🟩 🟢	🟩 🟢
		Power density	🟩	🟩 🟢	🟨 🟢	🟥 🟢	🟥 🟡	🟥 🟡	🟩 🟢	🟩 🟢	🟩 🟢
		Lifetime and stability	🟩	🟩 🔴	🟨 🔴	🟥 🔴	🟩 🟢	🟡 🔴	🟨 🟢 🔴	🟥 🔴	🟡 🔴
		Recyclability	🟩	🟩 🟢	🟩 🟢	🟩 🟢	🟩 🟢	🟩 🟢	🟩 🟢	N/A	🟡
	Value chain	Synthesis material losses	N/A	🔴	🟡		🟢	🟢	🟢	🔴	🔴
Energy Efficiency	Intrinsic	Device efficiency	🟩	🟩 🔴	🟨	🟥	🟥 🟡	🟥 🔴	🟩	🟥 🟡 🔴	🟡
	Value chain	Energy of nanosynthesis	N/A	🔴	🟡	🔴	🟡 🔴	🟡 🔴	🟡 🔴	🟢 🟡 🔴	🟡 🔴

Figure 3 Cathode materials for lithium ion batteries. Nanoarchitectured materials are given by a circle. Background colours reflect characteristics of bulk materials. Green denotes relative strength, red relative weakness, yellow intermediate characteristics, and white no data. Absence of circle indicates no data for nanomaterial. The grey background denotes the 'baseline' material. Abbreviations: NCA – lithium nickel cobalt aluminium oxide, NMC – lithium nickel manganese aluminium oxide, LCO – lithium cobalt oxide, LMR – lithium/manganese rich transition metal oxide, LFP – lithium iron phosphate, LVP - lithium vanadium phosphate, and LMO – lithium manganese oxide. Data from NCA from references [47,50,51,66,92,97,99,204,205]; data from NCM from references [33,46,50,51,60,66,97,98,204,206–209]; data from LCO from references [32,33,39,47,50,51,60,66,67,86,96,106,210,204,208,95]; data from LMR from references [47,50,51,60,66,97,98,101,204,211]; data from LFP from references [33,39,50–52,60,66,67,74,86,97,96,105–108,204,212]; data from LVP from references [50,51,60,66,86,97,109,213,214]; data from LMO from references [32,33,47,48,50,51,66,74,86,106,107,110,111,204,215]; data from S from references [47,50,51,56,60,86,93,112,116,118,120,216–231]; data from Li_2S from references [47,50,51,56,60,66,86,97,113,114,116,121,226,232,233]. See the Supplementary citation data for reference details.

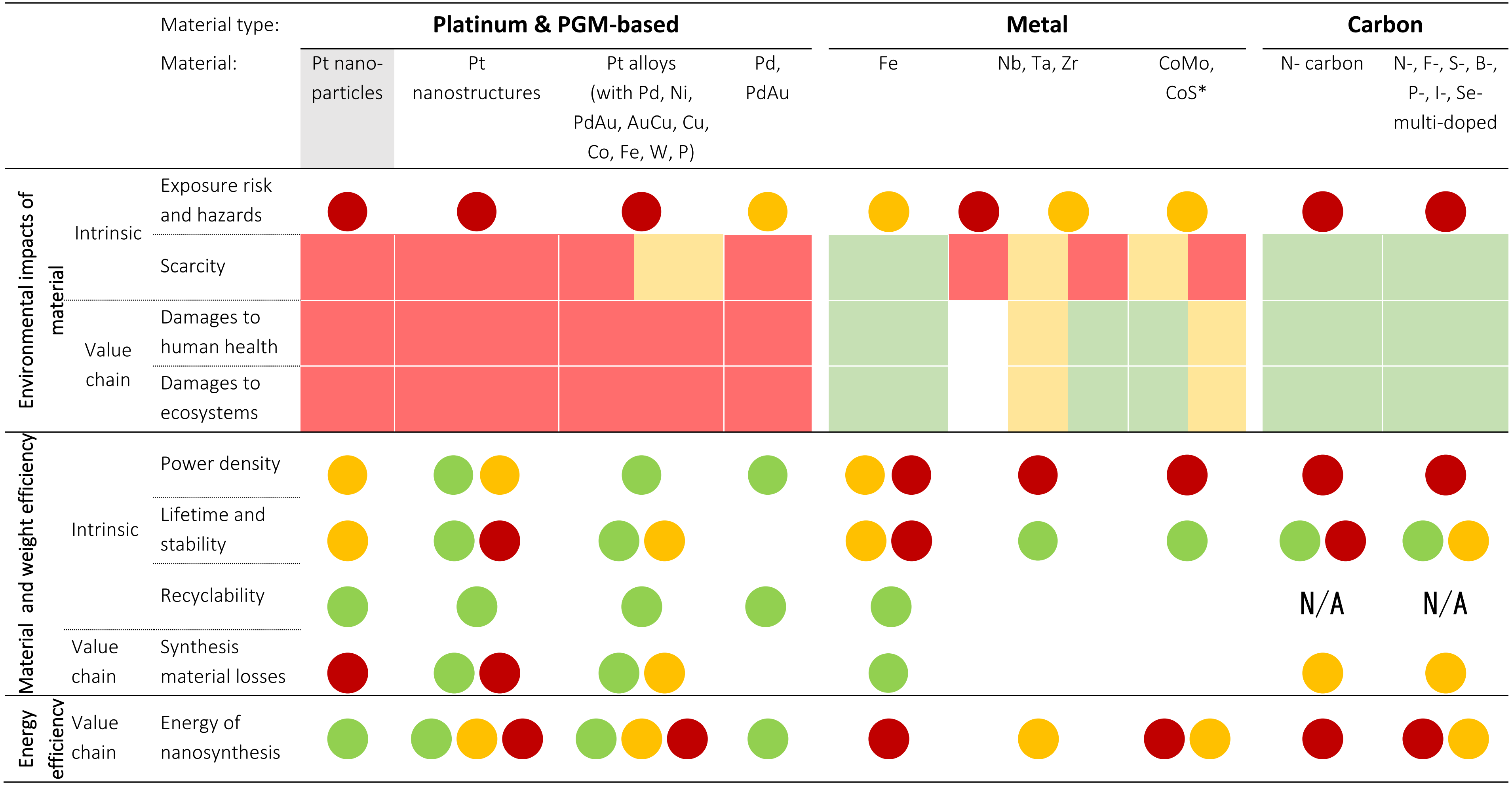

		Material type:	Platinum & PGM-based				Metal			Carbon	
		Material:	Pt nano-particles	Pt nanostructures	Pt alloys (with Pd, Ni, PdAu, AuCu, Cu, Co, Fe, W, P)	Pd, PdAu	Fe	Nb, Ta, Zr	CoMo, CoS*	N- carbon	N-, F-, S-, B-, P-, I-, Se- multi-doped
Environmental impacts of material	Intrinsic	Exposure risk and hazards	🔴	🔴	🔴	🟡	🟡	🔴 🟡	🟡	🔴	🔴
		Scarcity	🟥	🟥	🟥🟨	🟥	🟩	🟥🟨🟥	🟨🟥	🟩	🟩
	Value chain	Damages to human health	🟥	🟥	🟥	🟥	🟩	⬜🟨🟩	🟩🟨	🟩	🟩
		Damages to ecosystems	🟥	🟥	🟥	🟥	🟩	⬜🟨🟩	🟩🟨	🟩	🟩
Material and weight efficiency	Intrinsic	Power density	🟡	🟢 🟡	🟢	🟢	🟡 🔴	🔴	🔴	🔴	🔴
		Lifetime and stability	🟡	🟢 🔴	🟢 🟡		🟡 🔴	🟢	🟢	🟢 🔴	🟢 🟡
		Recyclability	🟢	🟢	🟢	🟢	🟢			N/A	N/A
	Value chain	Synthesis material losses	🔴	🟢 🔴	🟢 🟡		🟢			🟡	🟡
Energy efficiency	Value chain	Energy of nanosynthesis	🟢	🟢 🟡 🔴	🟢 🟡 🔴	🟢	🔴	🟡	🔴 🟡	🔴	🔴 🟡

Figure 4 Cathode catalyst materials for polymer electrolyte membrane fuel cells. Nanoarchitectured materials are given by a circle. Background colours reflect characteristics of bulk materials. Green denotes relative strength, red relative weakness, yellow intermediate characteristics, and white no data. Absence of circle indicates no data for nanomaterial. The grey background denotes the 'baseline' material. Abbreviations: PGM – platinum group metals, CoS - cobalt sulphur (on non-carbon black support). Data from Pt nanoparticles from references[47,50,51,60,66,177,234–237]; data from Pt nanostructures from references[47,50,51,60,66,137,138,177,234,236,238–243]; data from Pt alloys from references[47,50,51,60,66,133,139–144,177,234,236,242,244–258]; data from Pd and Pd alloys from references[47,50,51,60,177,236,252,259–261]; data from Fe from references[47,50,51,66,85,146,262,263]; data from Nb, Ta, Zr from references[47,50,51,60,66,264–269]; data from CoMo, CoS from references[47,50,51,60,66,270,271]; data from N-doped carbon from references[50,51,56,60,180,272–274]; data from N-, S-, B-, P-, I-, S-, Se- multi-doped carbon from references[50,51,56,147,149,275–279]. See the Supplementary citation data for reference details.

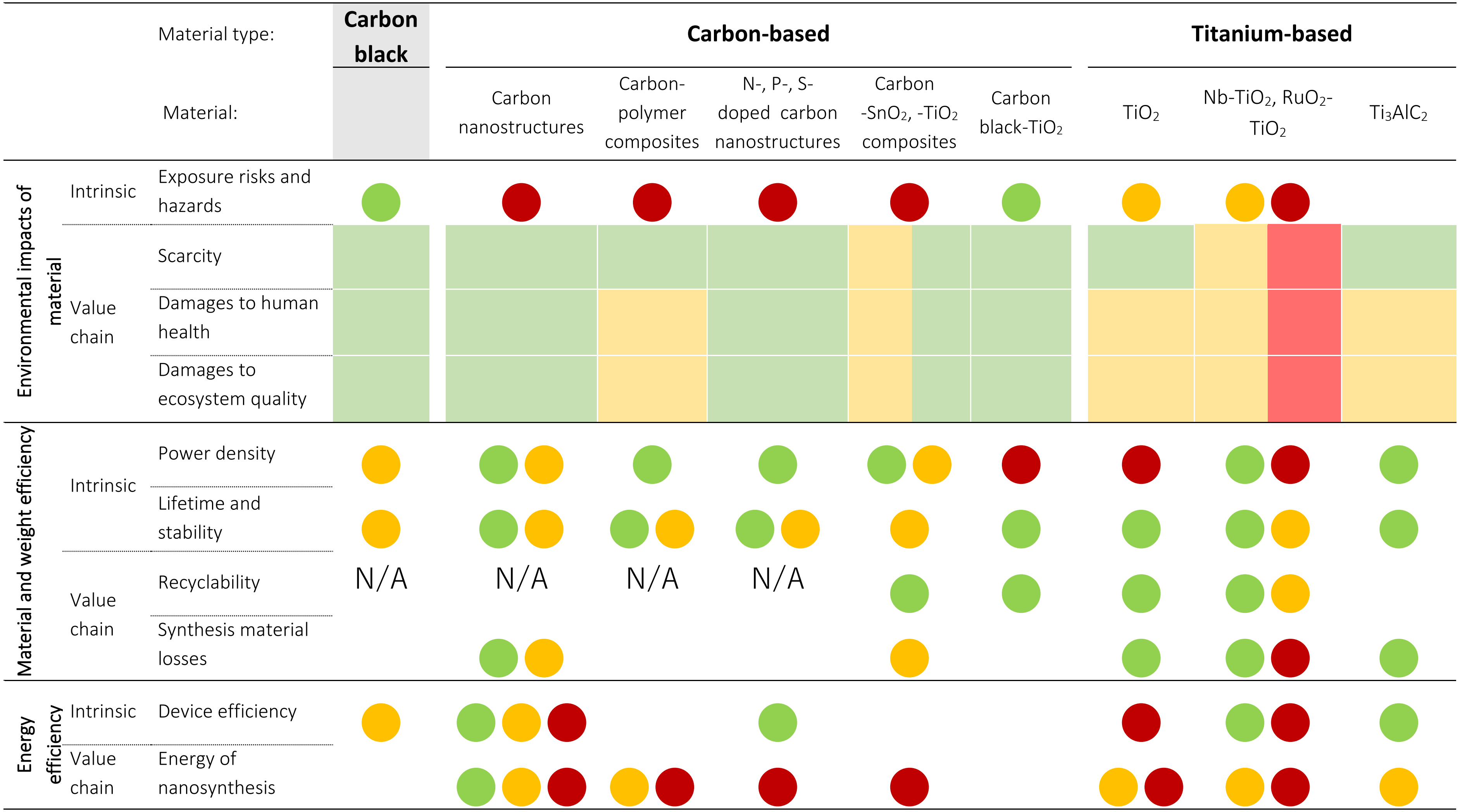

		Material type:	Carbon black	Carbon-based					Titanium-based		
		Material:		Carbon nanostructures	Carbon-polymer composites	N-, P-, S- doped carbon nanostructures	Carbon -SnO$_2$, -TiO$_2$ composites	Carbon black-TiO$_2$	TiO$_2$	Nb-TiO$_2$, RuO$_2$-TiO$_2$	Ti$_3$AlC$_2$
Environmental impacts of material	Intrinsic	Exposure risks and hazards	🟢	🔴	🔴	🔴	🔴	🟢	🟡	🟡 🔴	
	Value chain	Scarcity	🟩	🟩	🟩	🟩	🟨 🟩	🟩	🟩	🟨 🟥	🟩
		Damages to human health	🟩	🟩	🟨	🟩	🟨 🟩	🟩	🟨	🟨 🟥	🟨
		Damages to ecosystem quality	🟩	🟩	🟨	🟩	🟨 🟩	🟩	🟨	🟨 🟥	🟨
Material and weight efficiency	Intrinsic	Power density	🟡	🟢 🟡	🟢	🟢	🟢 🟡	🔴	🔴	🟢 🔴	🟢
		Lifetime and stability	🟡	🟢 🟡	🟢 🟡	🟢 🟡	🟡	🟢	🟢	🟢 🟡	🟢
	Value chain	Recyclability	N/A	N/A	N/A	N/A	🟢	🟢	🟢	🟢 🟡	
		Synthesis material losses		🟢 🟡			🟡		🟢	🟢 🔴	🟢
Energy efficiency	Intrinsic	Device efficiency	🟡	🟢 🟡 🔴		🟢			🔴	🟢 🔴	🟢
	Value chain	Energy of nanosynthesis		🟢 🟡 🔴	🟡 🔴	🔴	🔴		🟡 🔴	🟡 🔴	🟡

Figure 5 Catalyst support materials for polymer electrolyte membrane fuel cells. Nanoarchitectured materials are given by a circle. Background colours reflect characteristics of bulk materials. Green denotes relative strength, red relative weakness, yellow intermediate characteristics, and white no data. The grey background denotes the 'baseline' material. Abbreviation: N – nitrogen, P – phosphorus, S – sulphur, SnO$_2$ – tin oxide, TiO$_2$ – titanium oxide, CB-TiO$_2$ – carbon black-titanium oxide, Nb-TiO$_2$– niobium-doped titanium oxide, RuO$_2$-TiO$_2$ – ruthenium oxide-titanium oxide, Ti$_3$AlC$_2$ – titanium aluminium carbide. Data from carbon black from references[47,50,51,280]; data from carbon-based nanostructures from references [31,47,50,51,56,60,154,177,281–292]; data from carbon-based polymer composites from references[47,50,51,56,86,293–296]; data from carbon-based N-, P-, S- doped nanostructures from references[47,50,51,56,66,151,152,154,283,297–299]; data from carbon-based SnO$_2$, -TiO$_2$ composites from references[47,50,51,56,66,86,152,300–305]; data from carbon black -TiO$_2$ from references[47,50,51,66,304,305]; data from TiO$_2$ from references[47,50,51,66,300,304,306,307]; data from Nb-TiO$_2$ and RuO$_2$-TiO$_2$ from references[47,50,51,60,66,300,301,304,307–309]; data from Ti$_3$AlC$_2$from references[35,47,50,51,60,66]. See the Supplementary citation data for reference details.

Box 1 Life cycle assessment

Life cycle assessment (LCA) is an analytic method for estimating the environmental impacts associated with the production and consumption of products and services. This method first strives to inventory all exchanges with the environment necessary to deliver a function, considering the material and energetic inputs required at all stages, from raw material extraction, to processing and manufacturing, to product use, recycling, and final disposal. The total emissions and resource use associated with the delivery of a *functional unit* (e.g., transporting one person over one kilometre) are thus compiled in a lifecycle inventory. Examples of such emissions include carbon dioxide, methane, particulate matter and volatile organic carbons. These inventoried emissions are then linked to potential environmental *impacts,* such as climate change, eutrophication, acidification and ecotoxicity, using *characterization factors* determined by modelling, experimental results or physical properties. These potential environmental *impacts*, also referred to as *midpoint indicators*, may be further characterized based on their negative effects on key areas of protection, or *endpoint indicators*, as valued by humanity*: damage to human health, damage to ecosystems,* and *damage to resource availability*. Unfortunately, current characterization methods do not provide characterization factors for quantifying the impact of emissions of different nanomaterials in the environment. Nevertheless, despite data limitations and important sources of uncertainty, LCA provides a useful "whole system" perspective over entire supply chains. This perspective helps identify environmental "hotspots" and the processes where efficiency measures would have greatest effect.

<u>Supplementary information</u>

Leading the charge for environmentally sustainable electromobility with nanotechnology

Linda Ager-Wick Ellingsen, Christine Roxanne Hung, Guillaume Majeau-Bettez, Bhawna Singh, Zhongwei Chen, M. Stanley Whittingham , Anders Hammer Strømman

Contents

1. Relation of review framework to other methods and principles

The vast volume of literature focusing on nanomaterials relevant to lithium ion batteries (LIBs) and proton exchange membrane hydrogen fuel cells (PEMFCs) makes comprehensive life cycle assessments (LCAs) on all of these material candidates unrealistic. As the design phase of many products is decisive for their environmental lifecycle performance, integrating lifecycle thinking as early in the design phase as possible is important. In this review, we aim to introduce lifecycle thinking at an even earlier stage of product development. The text below describes how our framework relates to streamlined and full LCAs, the environmentally responsible product (ERP) qualitative matrix, and green chemistry.

Relation to streamlined and full life cycle assessments

The LCA standard defines a complete framework to quantify the environmental impacts associated with the production, use, and end-of-life of a product[1]. Such an approach is particularly relevant to the comparison of different products that deliver similar functions, which can serve to guide both product development and consumer choices. By quantifying multiple types of environmental burdens, such an assessment framework, minimizes the risks of problem shifting (in solving a problem, creating a new one) and unintended consequences.

The lifecycle screening method employed in this literature review is inspired by lifecycle assessment, but does not in itself constitute a full LCA.

Because LCAs strive to exhaustively inventory product systems from cradle to grave and to simultaneously cover a broad range of environmental burdens, such thorough assessments are generally considered to be data intensive, time consuming, and costly. This has raised concern as to the capacity of LCAs to guide the early design phase of products, since little data is typically available at this point and the full assessments of all possible design options would be prohibitively costly.

Such concerns are partly addressed by the iterative nature of the LCA process: it is recommended that LCAs start with a first estimate and progressively refine the assessment in dialogue with stakeholders or reviewers[1]. Several "streamlined LCA" methods have emerged to facilitate the elaboration of this first estimate, notably in the hope that it may provide timely guidance to influence product design. It has been argued that these simplified LCAs can be considered an integral part of the initial definition of the goals and the scope of a full assessment[2].

Strategies for streamlining LCAs include[2]:

1) Partly or fully ignoring upstream or downstream processes

2) Narrowing the range of environmental impacts considered

3) Limiting the constituents studied to those meeting a threshold volume

4) Using surrogate data

5) Mixing qualitative and quantitative data, depending on availability

6) Establishing "showstopper" criteria that render a certain option unacceptable and further analysis irrelevant

The present literature review of potential nanotechnological developments to LIB and PEMFC strives to synthesize what is known concerning the influence of their production, use, and end-of-life within all spheres of protection. It therefore avoids relying on strategies 1 and 2. This review focuses on the dominant material requirements and energy inputs to nanomaterial synthesis, to the partial exclusion of other requirements (e.g., infrastructure), following strategy 3. The evaluation of the different criteria relies on previous LCA reviews and generic data, following strategy 4. What is more, it regroups quantitative estimates into broad categories, along with more qualitative estimates, in agreement with strategy 5. The present screening does not rely on explicit "showstopper" criteria (strategy 6), but a certain number of thresholds are introduced beyond which a lifecycle parameter is considered problematic (see Section 3).

Beyond these common simplifying assumptions, the current review is distinct from an actual LCA due to its qualitative and semi-quantitative nature. As such, it closely related to the Environmentally Responsible Product (ERP) matrix, a screening tool also based on lifecycle thinking.

Relation to the Environmentally Responsible Product qualitative matrix

The ERP is a screening method that enables a rapid qualitative evaluation of a product's full lifecycle[3]. It is a particularly appropriate framework for producing an overall environmental profile for a broad range of products based on a review of sparse data, as we do in this literature review.

The ERP framework evaluates five broad environmental aspects that affect every stage of the lifecycle: the choice of environmentally responsible materials, the minimization of release of residues (solid, liquid and gaseous), and the reduction in energy use. We developed a framework that reflects the priorities that emerged from the LCA literature on EVs with some elements drawn from the ERP framework.

In the case of *material choice*, the ERP method focused on the avoidance of toxic, radioactive, restricted, scarce and virgin materials[4]. We refined this list of criteria to reflect today’s more abundant material LCA data and material hazard documentation. We screened the literature on the *exposure risks and hazards* of LIB and PEMFC materials, the potential *human health* and *ecosystems damages* caused by these materials' production chain, along with use of scarce resources. Together, these cover potential damage per mass of material to the three areas of protection (also called *endpoint indicators*) studied in LCAs[5], yielding an overall picture of the environmental intensity of the different materials.

Rather than focussing solely on *emissions of residues*, our analysis framework can account for all wastes and inefficient use of materials. In other words, in addition to examining waste of material through emissions, we also examined opportunities to fulfil the same function with less material, and the role that nanomaterials can play in this. Similarly, we expressed the *energy use* in terms of energy efficiency: achieving the same functionality with less energy inputs.

The ERP framework divides the lifecycle of products into five stages: *premanufacture*, *manufacture*, *packaging and transport*, *use*, and *end-of-life* (see rows in Supplementary Fig. 1). However, *packaging and transport* does not stand out as particularly relevant in recent LCAs of EVs and their powertrain devices, so this lifecycle stage was not addressed specifically in our framework. Similarly, it is difficult to distinguish between a *premanufacture* and a *manufacture* phase for nanomaterials. We therefore regrouped all three phases as the *production phase*, thereby simplifying the analysis.

For each nanomaterial, we strove to review the literature on its different lifecycle phases (rows) and lifecycle aspects (columns), presenting results in a three-category ranking (red – poor performance, yellow - intermediate, green – general improvement, as further detailed in Section 3. This is analogous to the qualitative approach by Graedel et al.[3], which ranked every parameter from 1 to 4.

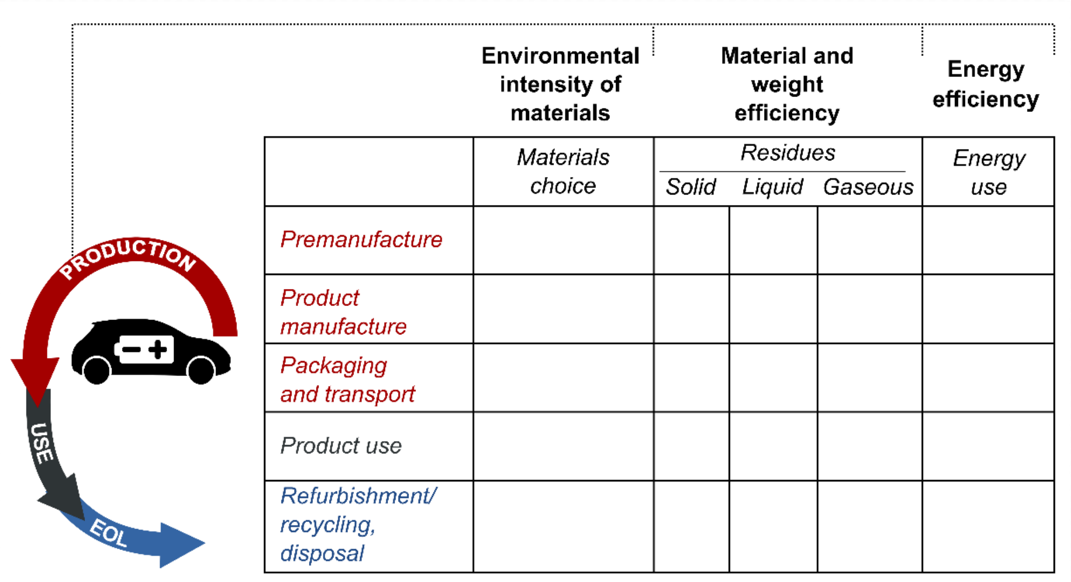

	Materials choice	Residues			Energy use
		Solid	Liquid	Gaseous	
Premanufacture					
Product manufacture					
Packaging and transport					
Product use					
Refurbishment/ recycling, disposal					

Supplementary Figure 1 Relation between our framework (bold text, outside table) and the Environmentally Responsible Product qualitative matrix (italic text, in table). *Coloured text in the first column shows how the lifecycle stages in the ERP correspond to those we consider in the review: red is production phase, dark grey is use phase and blue is end-of-life. Across the top row, the lifecycle sustainability strategies from this review and their corresponding criteria in the Environmentally Responsible Product matrix. Abbreviations: ERP - environmentally responsible product, EOL – end-of-life.*

Unlike the ERP framework, we strove throughout this review to distinguish between lifecycle aspects that stem from the intrinsic properties that the nanomaterials confer to the LIB and PEMFCs (e.g., energy density, cycling efficiency, etc.) and those that stem from the production chain (e.g., synthesis material losses, toxic emissions at the mine, etc.)

Relation to green chemistry

To ensure relevance in the daily reality of the chemistry and nanomaterial research communities, we link the various lifecycle aspects of our framework in the twelve principles of green chemistry[6,7] (see Supplementary Fig. 2).

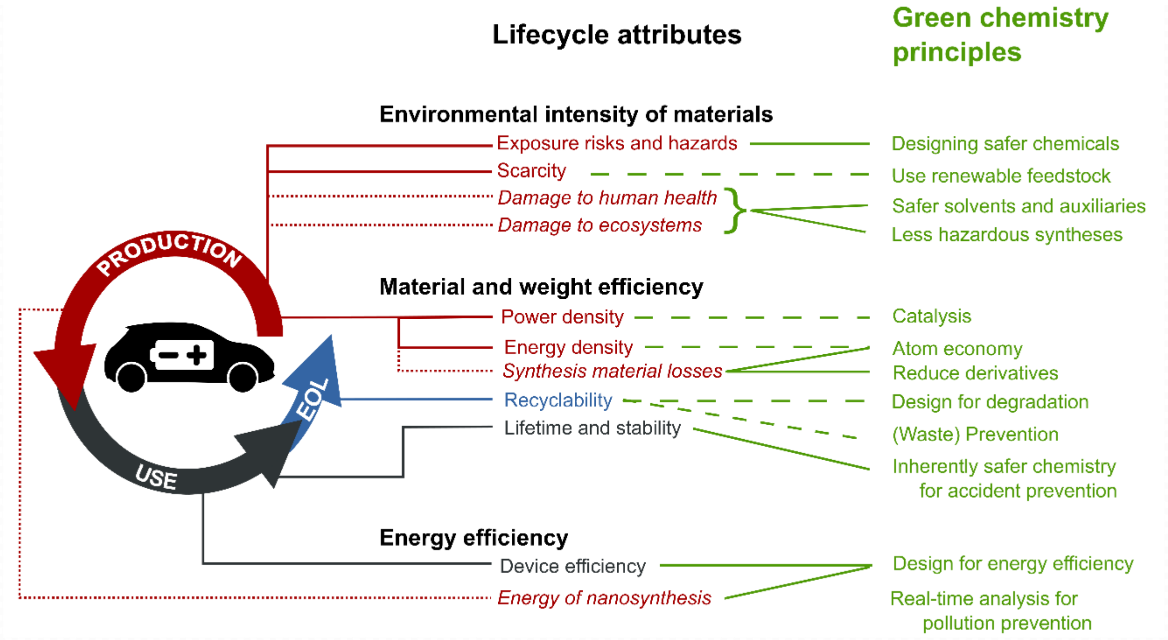

Supplementary Figure 2 Relation of lifecycle attributes to green chemistry principles. *Solid green lines denote clear correspondence between our review framework and the green chemistry principles, whereas dashed green lines denote* *partial correspondence. Solid lines denote intrinsic aspects pertaining to the material itself, whereas dotted lines with italic font denote properties that are attributes of the value chain or activities related to the material's production. Red lines denote production phase aspects, dark grey lines denote use phase aspects, and blue end-of-life aspects. Abbreviation: EOL – end-of-life.*

Multiple green chemistry principles are well aligned with the choice and production of materials with a lower environmental intensity. The aim of producing LIBs and PEMFCs that present lower exposure risks and hazards is in agreement with the principle of producing *chemicals that are safer by design*. Our focus on the use of less scarce resources in nanomaterial production is partly mirrored by the green chemistry goal of *using renewable feedstock*, although the use of metals is not in itself problematic if efficient recycling protocols are in place. Additionally, our focus on the human health and ecosystem damages in the materials production chain finds echoes in the search for *less hazardous syntheses* and *safer solvents and auxiliaries*.

A certain number of green chemistry principles also push for greater material efficiency, reinforcing our screening framework. Our review of synthesis material losses finds a direct counterpart in the concept of *atom economy*. By extension, the atom economy can also be understood as the aim of providing the same functionality with less mass, notably through gains in energy density in the case of LIBs. The predominant role of *catalyst development* in green chemistry is also highly relevant to the efforts to increase the power density of PEMFCs. Although none of the twelve green chemistry principles explicitly mention recyclability, the principle of *designing for degradation* and of *waste prevention* show a conscious planning for the end-of-life of the materials. Finally, the crucial question of the expected lifetime and stability of the LIB and PEMFCs finds a green chemistry counterpart with its preference for inherently *safer chemistry for accident prevention*.

Both our framework and the green chemistry principles clearly state the importance of *energy efficiency* for the environment.

2. Scope and resolution of review framework

The present framework strives to offer early insights into the parameters that may determine the environmental profile of nanomaterials in future LIBs and PEMFCs. To this end, the literature review must be guided by a framework that strategically covers the key aspects of these materials' lifecycles. We identify these aspects and justify the scope of our framework in relation to the sequential decomposition of the total impact of a technology (as illustrated in Supplementary Fig. 3).

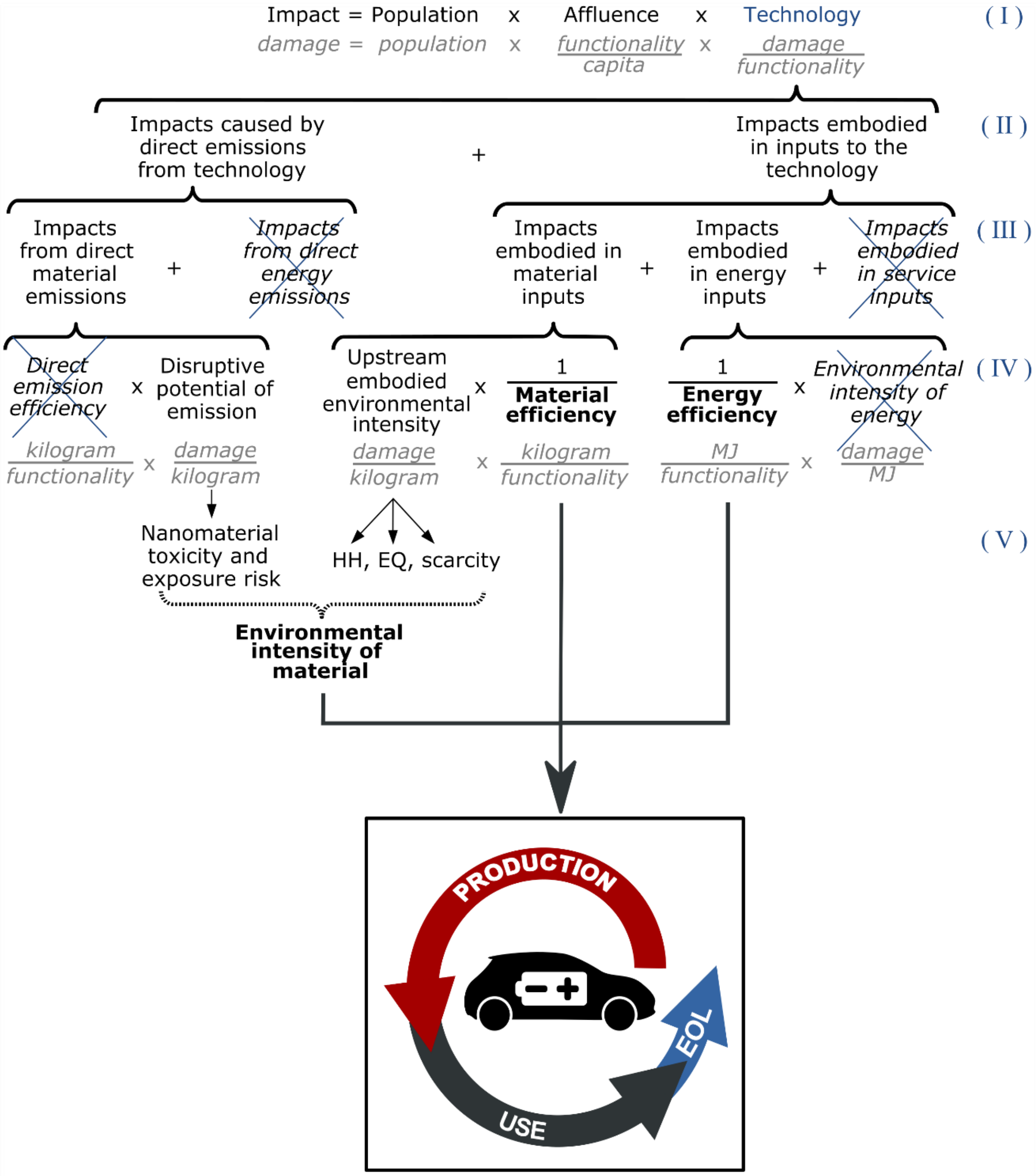

Supplementary Figure 3 ***Scope and resolution of review framework.*** *Terms in bold are the lifecycle attributes in our framework. Aspects that are crossed out are not considered in our framework. Grey text indicate the units of the terms in the decomposition. Abbreviation: MJ – megajoule, HH – human health, EQ - ecosystem quality, EOL – end-of-life.*

Perhaps the most famous and influential decomposition analysis is the so-called IPAT identity, which finds that our total environmental *Impact* can be understood as the product of the world *Population*, its level of *Affluence* (per-capita consumption), and the environmental intensity of the *Technologies* that satisfy this consumption (Supplementary Fig. 3, row I)[8]. The present literature review focuses on technologies that deliver a specific function (see *functional unit* in Box 1 in the main article); more specifically, that store and deliver energy for electromobility.

In analysing the total environmental impacts of a technology, it is often helpful to distinguish between, on the one hand, direct emissions released in the environment by the technology itself and, on the other hand, embodied emissions that occur in the value chains required by the technology (Supplementary Fig. 3, row II).

Pushing the decomposition further, it is common to categorize the inputs to a process, along with their embodied impacts. At a high level of aggregation, we can recognize three broad categories: material inputs (plastic, iron, etc.), energy inputs (electricity, heat), and services (transport services, infrastructure services etc.) (Supplementary Fig. 3, row III). We judged the last category to not be relevant for such early screening analysis, so impacts embodied in services were excluded from our scope, which is common practice, even in full LCAs[9]. Direct emissions can also be split between material releases in the environment and energy releases (waste heat, radiation, etc.), though the latter is not expected to be relevant to nanotechnological development.

It is common practice to decompose an environmental impact as the product between an amount and an environmental intensity[10]. Thus, the impacts embodied in a material input to a technology can be further decomposed as the product of two parameters: the amount of material needed by the technology to offer a functionality (kg of material per functionality) and the embodied environmental intensity of the material (embodied impacts per kg of material) (Supplementary Fig. 3, row IV). This is particularly relevant to nanomaterial synthesis, as nanotechnologies have the potential to change both the material efficiency of LIB and PEMFC, and the types of metals that enter in the production of these devices.

A similar decomposition can be performed for impacts embodied in energy use: it equals the amount of energy required multiplied by the upstream impacts per unit of energy (Supplementary Fig. 3, row IV). However, as most of the nanomaterials reviewed in the literature are not yet industrially produced, the locations of future industrial productions and the environmental intensity of the energy mix in these regions is not yet known. The environmental intensity of energy sources is therefore not relevant for the present analysis, only the amount of energy required (energy efficiency).

In a similar manner, impacts caused by direct emissions can be understood as the product between the amount of emissions and their capacity to cause damage in the environment per mass unit released (Supplementary Fig. 3, row IV). This early literature screening could not estimate direct material emissions during nanosynthesis or the battery use and recycling, so this was also excluded from the analysis.

The embodied environmental intensity is expressed following the three areas of protection, following common "endpoint" practice in LCA: human health, ecosystem quality, and scarcity[5]. As for direct emissions from nanosynthesis and use of nanomaterials, the literature review does not provide enough data to inventory the full range of potential emission types, and we restrict our analysis to the exposure risks and hazards of the nanomaterials themselves (Supplementary Fig. 3, row V). These four indicators for embodied and direct environmental intensities of materials are presented independently in our analysis but are thematically regrouped as describing the "environmental intensity of materials" involved in the lifecycle of nanotechnologies.

Thus, through typical decomposition of impacts and explicit scope restrictions, our analysis comes to articulate its review of nanomaterial around three lifecycle attributes (see rows in Figures 2-5 in main article). We review the literature for indications that nanomaterials might alter the material efficiency and energy efficiency of the manufacture, use, and end-of-life of LIBs and PEMFCs, along with the selection of materials with different lifecycle environmental intensities.

3. Criteria and basis for comparison

This literature review aims to cover a broad range of environmental parameters for a vast choice of potential nanomaterials that are in different stages of development. For many of these materials, the literature focuses much more on their electrochemical performance than on their overall environmental sustainability. This leads to wild variations in the availability and type of data in the literature, from precise quantitative measurements to qualitative descriptions, and also sometimes absence of data.

To consistently manage this diversity of data, we chose to represent all parameters in a semi-quantitative and a qualitative manner. For each parameter, we regrouped the different materials and processes in three categories (green, yellow and red in the article), ranking them from best to worst. This should allow for a thorough overview of the strengths and weaknesses of the different technologies, current trade-offs, potential hotspots, and avenues for improvements.

Working with a three-category semi-quantitative indicator ('red', 'yellow', and 'green' could equally well have been 1, 2, and 3) has multiple advantages for an early screening method. First, it can serve as a common denominator for combining differing data from a broad range of sources: quantitative measurement, qualitative descriptions, etc. Furthermore, restricting ourselves to three categories better reflects the high level of uncertainty that is associated with early environmental screening of lifecycle attributes of novel nanomaterials. Reporting scores on a finer scale, e.g., from 1 to 10 or even 1 to 100, would give a false sense of quantitative precision for many of the parameters reviewed.

The definition of these colour-coded categories was performed so as to represent the range of values reviewed for each parameter. However, the definition of the boundaries between the categories is necessarily partly subjective. This is an inherent difficulty associated with the definition of any classification scheme. To some extent, the reader must accept that the definition of classification criteria will be necessary until a fully quantitative LCA analysis is performed for all competing potential nanomaterials.

In this section, we strive to present explicit, clear, and reasonable rationale behind the ranking and classification of values for each environmental parameter. For some categories of impacts, we were able to leverage established ranking schemes with a similar level of resolution as our 3-category score (e.g., HMIS ranking). For parameters where quantitative data was consistently available, categories were determined by cluster analysis. For performance data, a commercial baseline was selected relative to which the different nanomaterials were evaluated, green denoting an improvement, yellow a similar performance, and red a deterioration. In other situations, thresholds were established based on the distribution of ranked (semi-quantitative) data, aiming for a balance in the number of materials in the green, yellow and red categories. In other words, if we rank data from best to worst, we defined thresholds to between categories so as to split the distribution in roughly equal parts. Finally, as a last resort, some thresholds were based on expert judgement in a few instances, as will be justified below.

This article's Supplementary citation data offers the interested reader all the necessary data to reorganize our review according to different classification criteria.

Environmental intensity of materials

Exposure risks and hazards

Exposure risks and hazards was assessed for materials using Material Safety Data Sheets (MSDS)[11] with the Hazardous Materials Identification System (HMIS) rating. The HMIS attempts to convey full health warning information to all employees and includes four sections: *Health, Flammability, Physical Hazard, and Personal Protection*[12]. With respect to *exposure risks and hazards,* only the *Health* section was deemed to be relevant. In the latest version of HMIS, there is an asterisk and a numeric health hazard rating. The asterisk signifies chronic health hazard, while the numeric health hazard signifies an acute health hazard. The asterisk health hazard is not always used[12]. Therefore, we use the numerical *Health* ratings, which are explained in Supplementary Table 1.

Supplementary Table 1 The numeric ranking system for the **Health** *according to the* **Hazardous Materials Identification System (HMIS).**

Health rating	HMIS health warning
4	Life-threatening, major or permanent damage may result from single or repeated overexposures.
3	Major injury likely unless prompt action is taken and medical treatment is given.
2	Temporary or minor injury may occur.
1	Irritation or minor reversible injury possible.
0	No significant risk to health.

In our review, all materials had *Health* rating below 3. Materials with a *Health* rating lower than 1 are 'green', between 1 and 2 'yellow', and 2 and higher 'red'. Carbonaceous nanostructures used as electrode materials in LIBs and catalyst support in PEMFCs were evaluated in their nanoform. HMIS health ratings were available for all of the LIB anode nanomaterials, except ruthenium oxide nanopowder. HMIS ratings of LIB intercalation cathode materials were only available for LCO and LMO. Ruthenium oxide, $LiNi_{1/3}Mn_{1/3}Co_{1/3}O_2$ (NMC), and $0.5Li_2MnO_3{\cdot}0.5LiNi_{1/3}Co_{1/3}Mn_{1/3}O_2$ (LMR) have HMIS health rating 2 (red) for bulk materials. We assumed that these materials would pose no less exposure risk in nanoform and therefore also rated the nanomaterials red. For compound materials and alloys where MSDSs were unavailable, constituent compound materials (e.g. sulphur nanoparticles and graphene for sulphur-carbon nanocomposites) or alloying metals (e.g. platinum and iron powders for PtFe) were combined to make a weight percent-based evaluation. We applied a precautionary principle and therefore, if any of the constituent materials received a red on its own, the alloy or compound was rated 'red'. Nanomorphologies were evaluating using MSDS for nanoparticle morphologies of the same material (with the exception of carbon nanostructures); for nanoalloys, the weighted average approach was used with the HMIS scores of the nanoparticle component elements.

Scarcity

Scarcity was assessed based on the long-term global resource availability of metals reported in the article "Criticality of metals and metalloids" by Graedel et al.[13] This indicator, which ranges between 0 and 100, takes into account the projected ore depletion times and the companion metal fraction in exploited ores. For the different metal alloys and compounds in nanomaterials, a mass-weighted scarcity score was calculated. The different metals and alloys involved in LIBs and PEMFCs were partitioned in the 'green', 'yellow' and 'red' groups by *k*-means clustering. This algorithm divides data into groups such that it minimizes the variance around the means in these groups[14], leading to representative and robust clusters of materials with similar supply risk scores.

Two expert judgement thresholds were nonetheless introduced in the analysis of scarcity. First, the analysis by Graedel et al.[13] does not include non-metals, such as silicon, carbon, and phosphorous. Because of their high abundance in the earth crust and ecosystems, all non-metals, including polymers, were judged to not be scarce and were assigned "green" scores.

Second, some metals that are not expected to represent a supply risk by Graedel et al.[13] are nonetheless extremely rare in the earth crust. We assigned to the "red" group any metal whose mass concentration in the earth crust is inferior to 50 parts per billion, which corresponds to the concentration of the 15 least abundant elements reviewed by Nitta et al.[15]. Our approach may then be seen as a "double bottom-line"; metals are assigned to the red group if they are assigned to this group by the *k*-means algorithm, or if their concentration in the earth crust falls below a threshold, or both. This reflects the conservative stance in view of the data uncertainty and the conceptual difficulty of defining and anticipating long-term scarcity issues[16,17].

The resulting graphs from the k-means clustering for the evaluated LIB and PEMFC materials are shown in Supplementary Fig. 4 and Supplementary Fig. 5, respectively.

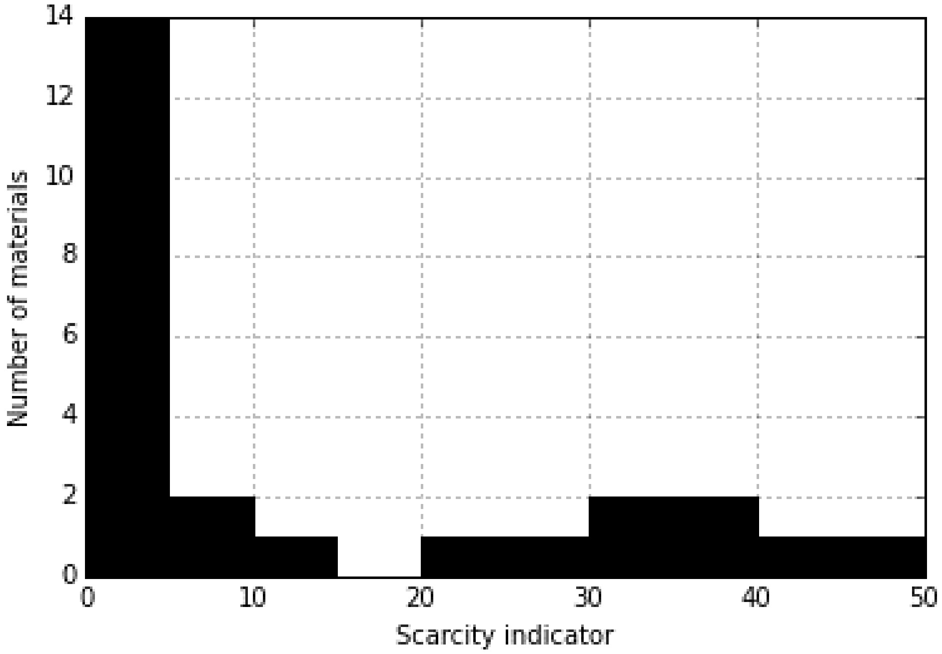

Supplementary Figure 4 Distribution of LIB materials by scarcity indicator score as in Graedel et al.[13].

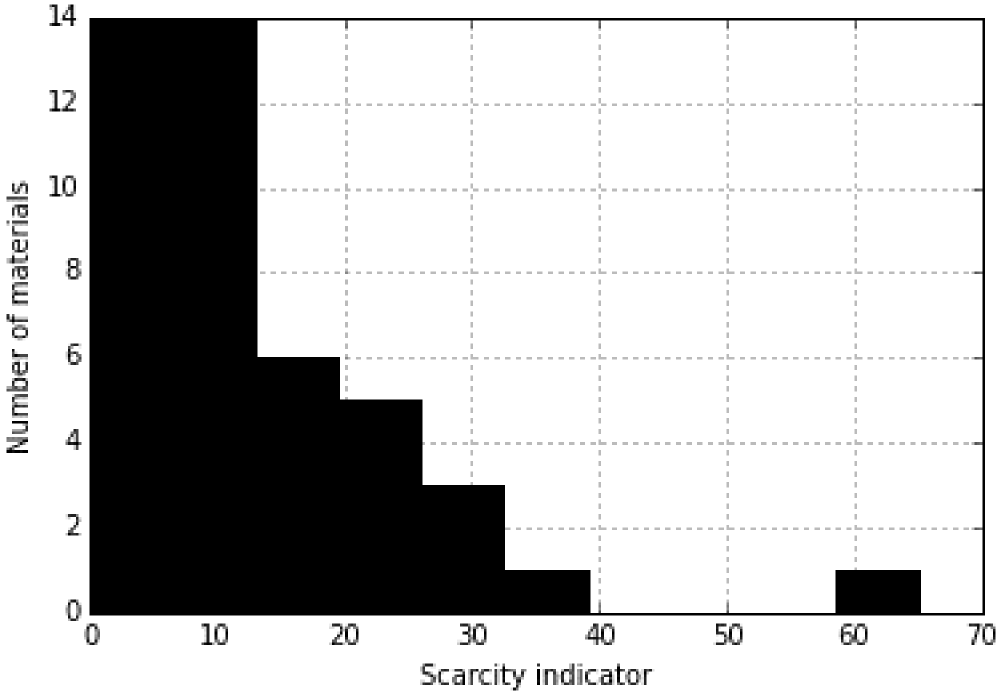

Supplementary Figure 5 Distribution of PEMFC materials by scarcity indicator score as in Graedel et al.[13].

Damage to human health and to ecosystems

Graedel et al.[13] evaluate *damages to human health* and *ecosystems* using *ecoinvent 2.2* and *ReCiPe 1.10* endpoint indicators from a hierarchical perspective for the production process of metals. In this review, we updated the results by using *ecoinvent 3.2* end *ReCiPe 1.11* and included non-metal materials used in LIBs and PEMFCs. For alloys and heterogeneous chemical compounds, the indicators were adjusted to match the stoichiometric composition of the alloy or compound, and presented per kg of alloy/heterogeneous compound.

As few metal oxides are represented in Graedel et al.[13] or in the *ecoinvent* database[18], all metals were compared based on the lifecycle impacts of their reduced form, for greater consistency across nanomaterials. Zirconium constitutes the only exception to this, as damage estimates were only available for the metal oxide.

In a similar manner as for the scarcity indicator, we employed *k*-means clustering to define the red, yellow and green material groups for embodied human health and ecosystem damages. However, the clustering was complicated by the large spread of impacts for the different materials, ranging over five orders of magnitude, from 10^{-6} to 10^{-1} DALY/kg in the case of embodied potential human health for fuel cell materials. This large spread lead to the quasi-totality of metals to be considered 'green', essentially because platinum and ruthenium have such disproportionately large impacts. Regrouping metals whose impacts range over orders of magnitude in the same (green) group would have been counterproductive. To regroup materials whose production impacts have a similar order of magnitude, we applied the *k*-means clustering to the $\log_{10}$ of the impacts. This allowed for the distinction not only of materials with extremely high impacts in the red group, but also materials with extremely low impacts in the green group.

The resulting graphs from the *k*-means clustering to the $\log_{10}$ of damages to human health and ecosystems caused by battery materials are shown in Supplementary Fig. 6 Supplementary Fig. 7, respectively.

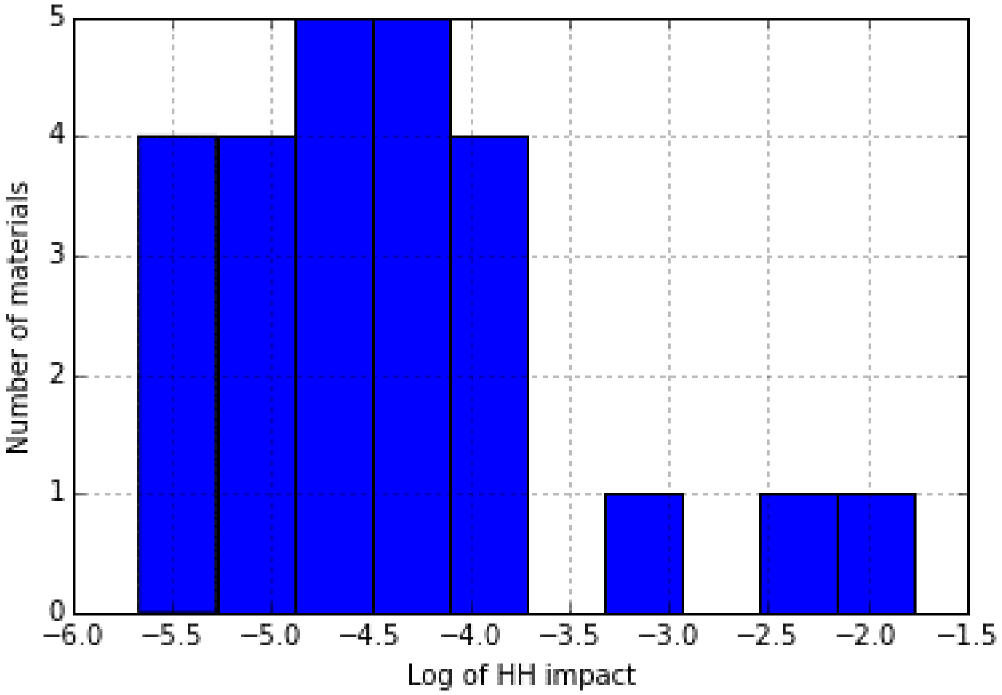

Supplementary Figure 6 Distribution of LIB materials by damages to human health indicator ($\log_{10}$ scale). *Abbreviation: HH – human health.*

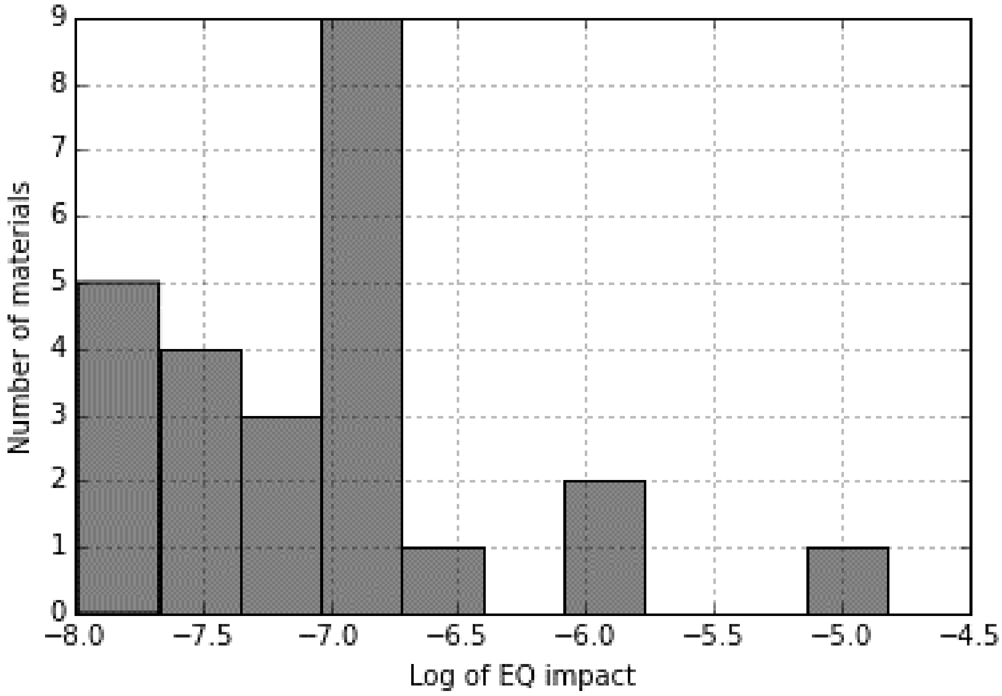

Supplementary Figure 7 Distribution of LIB materials by damages to ecosystem quality (log_{10} scale). *Abbreviation: EQ - ecosystem quality.*

The resulting graphs from the *k*-means clustering to the $\log_{10}$ of damages to human health and ecosystems caused by fuel cell materials are shown in Supplementary Fig. 8 and Supplementary Fig. 9, respectively.

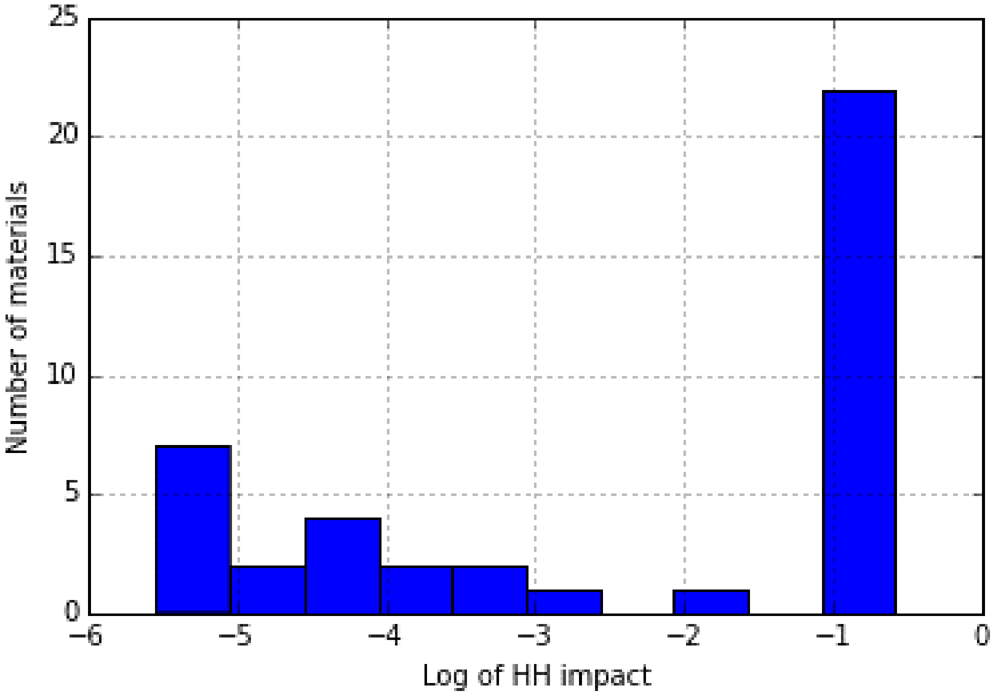

Supplementary Figure 8 Distribution of PEMFC materials by damages to human health indicator (log_{10} scale). *Abbreviation: HH – human health.*

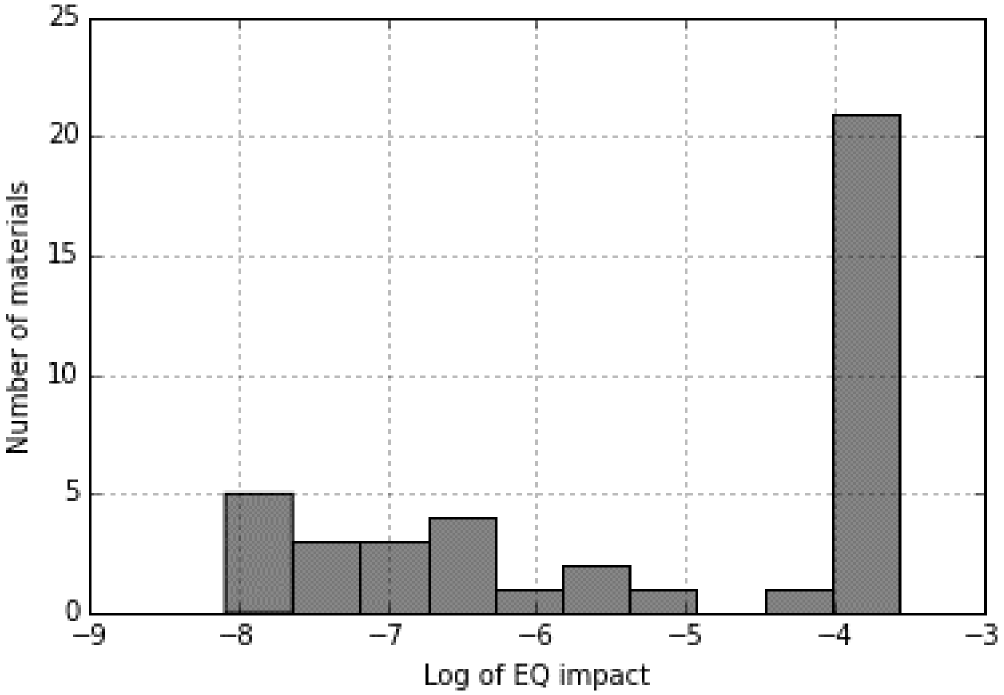

Supplementary Figure 9 Distribution of PEMFC materials by damages to ecosystem quality (log$_{10}$ scale). *Abbreviation: EQ - ecosystem quality.*

Material and weight efficiency

Energy density, power density, and lifetime and stability

To assess *energy density*, *power density*, and *lifetime and stability* aspects, we reviewed LIB and PEMFC literature. The abovementioned aspects were evaluated relative to the commercial "baseline", i.e. graphite (anode) and lithium nickel cobalt aluminium oxide (cathode) bulk materials for LIBs and nanoparticle platinum (catalyst) and high surface area carbon (catalyst support for PEMFCs. A general improvement is rated green, similar performance yellow, and poorer performance red. Supplementary Table 2 and Supplementary Table 3 list the performance parameters used to evaluate the *material and weight efficiency* criteria for LIBs and PEMFCs, respectively.

Supplementary Table 2* Material and weight efficiency *criteria for lithium ion batteries. *Abbreviations: mAh g-^{1} – milliampere-hour per gram, V – voltage, kWh kg-^{1} – kilowatt-hour per kilogram.*

LIBs	Energy density	Power density	Lifetime and stability
Cathode and anode materials	• Capacity (mAh g^{-1}) • Voltage (V) • Energy density (kWh kg^{-1})	• Rate capability/ performance/characteristics • Rate of lithium intercalation/deintercalation • Conductivity • Impedance	• Calendar/cycling life • Capacity fade/loss • Stability (thermal, structural, and cycling) • Performance degradation • Failure • Fade in charge storage • Reaction with the electrolyte • Number of cycles • Cyclability • Cycling performance • Coulombic efficiency

Supplementary Table 3 **Material and weight efficiency *criteria for proton exchange membrane fuel cells.*** *Abbreviations: PEMFCs - proton exchange membrane hydrogen fuel cells, A cm^{-2} – ampere per square centimetre, A mg$^{-1}{}_{Pt}$ – ampere per milligram platinum, A mg$^{-1}{}_{Pt}$ – ampere per milligram catalyst, V – voltage, W cm^{-2} – watt per square centimetre, ECSA – electrochemical surface area, H_2O_2 – hydrogen peroxide.*

PEMFCs	Power density	Lifetime and stability
Cathode catalyst & support	• Current density (A cm^{-2}, A mg$^{-1}{}_{Pt}$, A mg$^{-1}{}_{catalyst}$) • Generated voltage (V) • Power density (W cm^{-2}) • Oxygen reduction reaction kinetic rate • Onset voltage • ECSA	• ECSA retained after accelerated durability testing • H_2O_2 evolution rate • Polarization shift • Loss of current, power density

The relevant literature are referred to in the text and the caption of Figures 2-5 in the main article and in greater detail in the *Supplementary citation data*.

Recyclability and disposal

The recyclability of the studied LIB electrode materials and PEMFC materials was assessed based on current recycling practices as described in the literature[19–24] and through personal communication with commercial recylers[25,26] of these devices. Materials that can be reused or recycled receive a green ranking, materials that are unproblematic for disposal or have "imperfect" recycling processes receive a yellow ranking, and materials that may pose issues at the end-of-life processing receive a red ranking. N/A was assigned to materials where recycling is not a priority, e.g., for materials where there is no foreseeable shortage, such as sulphur or renewables. Material and energy inputs required for the various recycling processes were not assessed. For LIBs, the recyclability of nanoscale materials was assumed to be similar to that of the bulk materials.

Synthesis material losses

Synthesis material losses were evaluated based on synthesis protocols available in the literature, as well as synthesis reviews describing environmentally significant aspects[27–30]. Because bottom-up methods allow for the customized design of reactions and processes at the molecular level and thereby minimizing unwanted waste, it is generally believed that top-down techniques are more waste-producing than bottom-up techniques[29].

The solvothermal synthesis methods are environmentally advantageous, as rates of reactions are increased (closed system) and reagents are recycled[29]. The method is called hydrothermal if the used solvent is water[27]. Sonochemical synthesis is also environmentally advantageous, with yields as high as 90-95% due to ultrasonic irradiation[29,31]. Milling is said to be a highly efficient and low emission method[30]. The solid state synthesis method has high economic efficiency[30], suggesting low use of costly solvents and high production yields resulting in low synthesis material losses. Electrospinning is said to be a "green" and facile route that can easily be scaled up and is a low cost process[30], again suggesting low material losses.

Utilization efficiency of a plasma enhanced chemical vapour deposition (CVD) chamber ranges from 5% to 62%, depending on what perfluorocarbon is used[29]. It is environmentally preferable to thermal CVD as it operates at lower temperatures and has a higher production yield[27]. Yield values of carbon nanotubes production by the CVD method vary from 20% to 100%[29]. Although carbon nanotubes can be produced via four major synthesis routes (arc discharge, CVD, laser ablation, and the high pressure carbon monoxide process)[32], CVD is the only promising synthesis method for large scale production[27].

In this review, it was assumed that carbon nanotubes is synthesised through the CVD method with mediocre synthesis yield. Laser ablation synthesis yield range up to 70%[29].

Nanoparticles extracted from solution by precipitation must be washed repeatedly with organic solvents and ultrapure water until the products are isolated from solvents, surfactants, or reagents[29]. The precipitation method employs heavy chemical usage pre- and post-synthesis for purifying the product and accompanying wastewater generation from centrifugation or other separation techniques[29]. Sol-gel offers control over purity, composition, homogeneity and temperature, but it also requires large amount of organic solvents and reagents[30] and has low yield[29]. Metal organic CVD is a high cost route[30] that has a low precursor utilization efficiency of only 1 to 20% and at least 50% of the precursor gases becomes waste[29]. Wet etching use strong acids, metal salts, and generates acidic or organic waste, whereas dry etching uses greenhouse gases with low utilization efficiency[29]. Arc discharge synthesis has low yields hovering around 30%[29].

Supplementary Table 4 shows a general evaluation of *synthesis material losses* for nanosynthesis methods reviewed in this article.

Supplementary Table 4 Overview of* Synthesis material losses *for nanomaterials synthesis routes reviewed in this article. *Abbreviation: CVD - chemical vapour deposition.*

	Green	Yellow	Red
Synthesis material losses (nanomaterial purity, yield)	• Solvothermal/hydrothermal • Sonochemical • Milling • Solid state • Electrospinning	• Plasma enhanced CVD • CVD for carbon nanotubes • Laser ablation	• Precipitation • Sol-gel • Metal organic CVD • Etching • Arc discharge

Energy efficiency

Device efficiency

The device efficiency was evaluated relative to the commercial “baseline”, i.e. graphite and lithium nickel cobalt aluminium oxide (NCA) bulk electrode materials for LIB and Nafion® membrane for PEMFCs. In LIBs, device energy efficiency was evaluated based on Coulombic efficiency and cycling (charge-discharge) efficiency. Vehicle batteries must have a Coulombic efficiency exceeding well over 99.5% if their effective lifetime is to exceed five years. LCA studies analysing LIBs apply charge-discharge cycling efficiencies of 90%[33–36] and 95-96%[37]. The cathode material cycling efficiency can be nearly 100%, whereas the carbonaceous (graphite) anode shows initial efficiency of 95% and lower[38]. In addition to stated cycling efficiencies, the efficiency was evaluated based on voltage hysteresis and factors contributing to internal resistance, such as phase transition, material polarization, electrical conductivity, and structural change. In PEMFCs, device energy efficiency is evaluated on the basis of internal resistance in the cell, and (for the components considered in the review) is determined by the electrical conductivity of the catalyst supports.

Energy of nanosynthesis

Energy of nanosynthesis is a measure of how much energy was required to produce a certain nanomaterial. Similar to the evaluation of *synthesis material losses*, *energy of nanosynthesis* was evaluated based on synthesis protocols and synthesis reviews describing environmentally significant aspects[27–30]. In some cases, the nanosynthesis method in itself may not be particularly energy demanding, but can require subsequent drying heat for annealing or calcination, which may be significant. Therefore, energy of nanosynthesis evaluations are seen as combination of synthesis methods and temperatures. The text below describes relevant energy use for some synthesis processes.

Despite long synthesis times, sonochemical synthesis is a low-energy synthesis route as it takes place at room temperature[31] and only requires energy for ultrasonic irradiation and any baths or probes that are used[29]. Chemical etching can be performed near room temperature[39]. Wet etching requires energy for agitation, whereas plasma etching requires energy for plasma and vacuum system[29].

Plasma-enhanced CVD requires energy for the plasma generator and vacuum system and requires significantly lower temperature than the CVD process[27]. Hydrothermal and solvothermal are low-temperature synthesis routes and may be preferred as they are not as energy intensive as other methods[27,29,40,41] and do not require post-annealing treatments[29]. The hydro- and solvothermal operation temperatures are usually between 100-280 °C[41] for 5-10 hours[28]. Calcination temperatures are lower (e.g. 400-750 °C for 0.5-12 hours[28]) compared to the solid-state methods. Energy use for electrospinning itself is associated only with high-voltage power supply and syringe pump[29] as it may be performed at room temperatures[42], but the subsequent calcination requires high temperatures of about 500-900 °C[42,43]. Even though the mechanical milling process only requires energy for the milling equipment and can work at low temperatures[27], high-energy mechanical milling requires high temperatures for calcination (e.g. 400-700 °C for silicon-carbon composites)[29,30]. It is therefore considered as a rather energy intensive process[44].

Metal organic CVD takes place at higher temperatures than plasma-enhanced CVD; its primary energy consumption is associated with the vacuum system (low to medium vacuum pressure range: 0.5 to 760 Torr), gas handling system, purifiers, heat treatment of reactants before deposition, and high deposition temperatures (500-1200 °C)[27,29]. Nanosynthesis through precipitation and co-precipitation requires energy for heating treatments[28], such as drying and calcination[29]. Calcination temperatures of 500-800 °C for 12 hours under N_2 or argon flow is required for the crystalline LFP powders[28], but higher temperatures have also been reoported[45,46]. Sol-gel is a long established industrial process for producing nanoparticles[27] and is often used for the preparation of metal oxides[28]. The sol-gel process itself can be performed at low temperatures, but requires drying and subsequent furnace treatment (e.g. LTO is calcined at 700-800 °C[30]) under an inert or reducing atmosphere[40]. Solid state synthesis is a technique used to produce chemical structures by reactions carried out at extreme conditions, such as high temperature and pressure. Prepared mixtures are often heated in two steps. For LFP, the first step is carried out at 250-350 °C and the second step at 400-800 °C[28]. In general, the appropriate sintering temperature range is 650–700 °C[28]. Calcination temperatures as high as 800-1000 °C are also used[30]. Arc discharge is a very high energy synthesis route, employing processing temperatures above 4000 °C. Spray pyrolysis typically starts with the pumping (or spraying) of a solution of mixed precursors into a pyrolysis furnace at moderate temperatures ranging between 100–600 °C in the form of droplets by a carrier gas[28,47]. The collected precursor powders are then annealed at temperatures typically ranging between 400–800 °C[28,47]. As there is such a great span in temperature ranges, the energy requirements of spray pyrolysis may be moderate or high.

Synthesis and processing routes for nanomaterials were roughly evaluated qualitatively considering the required processing temperature input as described specifically in the synthesis protocols or more generally regarding synthesis methods. Due to large variation in temperature, pressure, and duration of treatment, the evaluation of energy of nanosynthesis is more prone to uncertainty than other aspects evaluated in this review. Furthermore, as the nanomaterials may be synthesized through different synthesis routes, the evaluation was limited to the synthesis routes reviewed in this article. As previously mentioned, carbon nanotubes can be manufactured using various synthesis methods. Carbon nanotubes manufacturing is energy intensive regardless of synthesis method, but arc discharge and laser ablation are more energy intensive than CVD and the high pressure carbon monoxide process[32]. Production of carbon nanotubes was therefore always rated as red.

Supplementary Table 5 shows a general evaluation of *energy of nanosynthesis* for nanosynthesis methods reviewed in this article.

Supplementary Table 5 Energy of nanosynthesis evaluation for some synthesis routes. *Abbreviation: CVD - chemical vapour deposition.*

	Green	Yellow	Red
Energy of nanosynthesis	• Sonochemical • Etching	• Plasma enhanced CVD • Solvothermal/hydrothermal • Electrospinning • Milling • Spray pyrolysis (low temperatures)	• Metal organic CVD • Precipitation • Sol-gel • Solid state • Arc discharge • Spray pyrolysis (high temperatures)

4. Review of bulk polymer matrices for electrolyte membranes

The following is a review of the main groups of polymer electrolyte membranes for PEMFCs. These polymers are bulk materials whose main functionality (i.e., proton conduction) occurs on the nanoscale. Since the main article reviews nanotechnology modification to these polymers, the bulk materials are briefly evaluated here using the lifecycle attributes to provide relevant background information to be considered in parallel with the main text. Keeping in mind our lifecycle sustainability attributes, we differentiate between two main membrane material categories: fluorinated and non-fluorinated membranes.

Fluorinated membranes may be fully fluorinated, such as Nafion (poly(perfluorinated sulfonic acid); PFSA), or partially fluorinated polymers. To date, these membranes have the best technical performances in operating PEMFCs, but device efficiency (proton conductivity) decreases at higher temperatures and in anhydrous conditions[48]. Work has therefore aimed at finding materials and means of improving existing materials under these conditions. Promising low equivalent-weight PFSA membranes such as perfluoroimide acids have greater ionic conductivity per gram of polymer and thus provide increased power density than Nafion. These materials also show improved device efficiency and lifetime over conventional Nafion in hot and dry operating conditions, through greater proton conductivity and stability, respectively[49]. Partially fluorinated membranes based on polymers such as polyvinylidene fluoride and poly(ethylene-*co*-tetrafluoroethylene) lack the durability and tolerance to fuel impurities to be considered in transport PEMFCs, despite their oxidative stability[50].

The specific toxicological effects, bioaccumulation and biomagnification tendencies and exposure risk of the fluorinated polymers being explored as PEMFC membranes do not appear to have been studied. Similar fluorinated polymers such as perfluoroalkyl carboxylic and sulfonic acids, however, are found to be persistent and bioaccumulative, and, in some cases, biomagnified[51,52]. Furthermore, chemical degradation of fluorinated membranes during PEMFC operation result in the release of corrosive and toxic hydrofluoric acid[48,53], which is also a precursor to the fluorinated polymers. Tetrafluoroethylene, another precursor to fluorinated polymers, is also of toxicological concern[54]. As such, from the perspective of material impacts, it is highly recommended to focus research on the pursuit of non-fluorinated PEMFC membranes.

Non-fluorinated membranes include acid and hydrocarbon membranes such as poly(arylene ether)s, polyimides, styrene and derivatives, as well as inorganic or solid acid membranes (e.g., $CsHSO_4$, $Rb_3H(SeO_4)_2$ and heteropolyacids such as $H_3PW_{12}O_{40}.nH_2O$, etc). These membranes have generally fallen short of the technical goals for PEMFCs for transport applications; they have lower device efficiency due to their lower ionic conductivity, or are unstable and lack the robustness required for an adequate device lifetime relative to Nafion membranes[50,55]. However, as discussed above, their lack of fluorine atoms generally makes these materials less environmentally intensive than fluorinated membranes and modifications such as covalent attachment of proton-conductive compounds, cross-linking and nanostructure are being explored as methods to overcome weaknesses[49,56–60]. An exception to the technical performance of this category of membranes are phosphoric acid-doped polybenzimidazole-based membranes. These membranes perform well in high temperatures with low humidity levels and are robust against fuel impurities. However, they also have reduced device lifetime due to lower mechanical strength and due to damage caused by phosphoric acid leachate formed under normal operating conditions; acid leaching also decreases the energy efficiency of the membrane via losses in proton conductivity[58,61]. Beyond the attributes considered here, phosphoric acid-PBI membranes may have issues with cold start due to poor device efficiency performance at lower temperatures.

Composite membranes have been researched as a synergetic means to boost the performance of two or more different polymers. In addition to the composite electrospun membranes discussed in the main manuscript, polytetrafluoroethylene-reinforced PFSA membranes demonstrate improved lifetime characteristics and device efficiency over benchmark Nafion membrane[48]. The mechanical strength provided by the polytetrafluoroethylene matrix improves material efficiency by allowing thinner membranes, which also improves the device energy efficiency by reducing ionic resistance.

References

1. Guinée, J. *Handbook on Life Cycle Assessment: Operational Guide to the ISO Standards*. (Springer Netherlands, 2002).
2. Todd, J. A. & Curran, M. A. Streamlined Life-Cycle Assessment: A Final Report from the SETAC North America Streamlined LCA Workgroup. *Environ. Toxicol.* 31 (1999).
3. Graedel, T. E., ALLENBY, B. R. & COMRIE, P. R. Matrix Approaches to Abridged Life Cycle Assessment. *Environ. Sci. Technol.* **29,** 134A–139A (1995).
4. Graedel, T. E. *Streamlined life-cycle assessment*. (Prentice Hall, 1998).
5. Hauschild, M. Z. *et al.* Identifying best existing practice for characterization modeling in life cycle impact assessment. *Int. J. Life Cycle Assess.* **18,** 683–697 (2013).
6. Anastas, P. T. & Warner, J. C. *Green Chemistry: Theory and Practice*. (Oxford University Press, 1998).
7. Anastas, P. T. & Eghbali, N. Green Chemistry: Principles and Practice. *Chem. Soc. Rev.* **39,** 301–312 (2010).
8. Chertow, M. R. The IPAT Equation and Its Variants. *J. Ind. Ecol.* **4,** 13–29 (2000).
9. Majeau-Bettez, G., Strømman, A. H. & Hertwich, E. G. Evaluation of Process- and Input–Output-based Life Cycle Inventory Data with Regard to Truncation and Aggregation Issues. *Environ. Sci. Technol.* **45,** 10170–10177 (2011).
10. Minx, J. C. *et al.* A ‘ Carbonizing Dragon ’: China ’ s Fast Growing CO 2 Emissions Revisited. 9144–9153 (2011).
11. Titanium Industries. *Material Safety Data Sheet For Titanium Metal*. (2013).
12. The MSDS HyperGlossary: HMIS. Available at: http://www.ilpi.com/msds/ref/hmis.html. (Accessed: 11th April 2016)
13. Graedel, T. E., Harper, E. M., Nassar, N. T., Nuss, P. & Reck, B. K. Criticality of metals and metalloids. *Proc. Natl. Acad. Sci.* **112,** 4257–4262 (2015).
14. Lloyd, S. P. Least Squares Quantization in PCM. *IEEE Trans. Inf. Theory* **28,** 129–137 (1982).
15. Nitta, N., Wu, F., Lee, J. T. & Yushin, G. Li-ion battery materials: present and future. *Mater. Today* **18,** 252–264 (2015).
16. Gordon, R. B. B., Bertram, M. & Graedel, T. E. E. On the sustainability of metal supplies: A response to Tilton and Lagos. *Resour. Policy* **32,** 24–28 (2007).
17. Tilton, J. E. & Lagos, G. Assessing the long-run availability of copper. *Resour. Policy* **32,** 19–23 (2007).
18. Ecoinvent Centre. *Ecoinvent data and reports 3.2*. (2015).
19. Handley, C., Brandon, N. P. & Van Der Vorst, R. Impact of the European Union vehicle waste directive on end-of-life options for polymer electrolyte fuel cells. *J. Power Sources* **106,** 344–352 (2002).
20. SHIROISHI, H. *et al.* Electrochemistry. *Electrochemistry* 7–12 (2012).
21. Xu, F., Mu, S. & Pan, M. Recycling of membrane electrode assembly of PEMFC by acid processing. *Int. J. Hydrogen Energy* **35,** 2976–2979 (2010).
22. Xu, J. *et al.* A review of processes and technologies for the recycling of lithium-ion secondary batteries. *J. Power Sources* **177,** 512–527 (2008).

23. Hanisch, C., Diekmann, J., Stieger, A., Haselrieder, W. & Kwade, A. Recycling of Lithium-Ion Batteries. *Handb. Clean Energy Syst.* 1–24 (2015). doi:10.1002/9781118991978.hces221

24. Hanisch, C. *et al.* Recycling of lithium-ion batteries: a novel method to separate coating and foil of electrodes. *J. Clean. Prod.* **108,** 301–311 (2015).

25. Accurec. Personal communication. (2016).

26. Umicore. Personal communication. (2015).

27. Charitidis, C. a., Georgiou, P., Koklioti, M. a., Trompeta, A.-F. & Markakis, V. Manufacturing nanomaterials: from research to industry. *Manuf. Rev.* **1,** 11 (2014).

28. Satyavani, T. V. S. L., Srinivas Kumar, A. & Subba Rao, P. S. V. Methods of synthesis and performance improvement of lithium iron phosphate for high rate Li-ion batteries: A review. *Eng. Sci. Technol. an Int. J.* **19,** 178–188 (2015).

29. Şengül, H., Theis, T. L. & Ghosh, S. Toward Sustainable Nanoproducts. *J. Ind. Ecol.* **12,** 329–359 (2008).

30. Lee, W. W. & Lee, J.-M. Novel synthesis of high performance anode materials for lithium-ion batteries (LIBs). *J. Mater. Chem. A* **2,** 1589–1626 (2014).

31. Arvidsson, R., Kushnir, D., Sandén, B. a & Molander, S. Prospective life cycle assessment of graphene production by ultrasonication and chemical reduction. *Environ. Sci. Technol.* **48,** 4529–36 (2014).

32. Upadhyayula, V. K. K., Meyer, D. E., Curran, M. A. & Gonzalez, M. a. Life cycle assessment as a tool to enhance the environmental performance of carbon nanotube products: A review. *J. Clean. Prod.* **26,** 37–47 (2012).

33. Majeau-Bettez, G., Hawkins, T. R. & Strømman, A. H. Life cycle environmental assessment of lithium-ion and nickel metal hydride batteries for plug-in hybrid and battery electric vehicles. *Environ. Sci. Technol.* **45,** 4548–54 (2011).

34. Kushnir, D. & Sandén, B. a. Energy requirements of carbon nanoparticle production. *J. Ind. Ecol.* **12,** 360–375 (2008).

35. Lastoskie, C. M. & Dai, Q. Comparative life cycle assessment of laminated and vacuum vapor-deposited thin film solid-state batteries. *J. Clean. Prod.* **91,** 158–169 (2015).

36. Zackrisson, M., Avellan, L. & Orlenius, J. Life cycle assessment of lithium-ion batteries for plug-in hybrid electric vehicles - Critical issues. *J. Clean. Prod.* **18,** 1519–1529 (2010).

37. Ellingsen, L. A.-W. *et al.* Life cycle assessment of a lithium-ion battery vehicle pack. *J. Ind. Ecol.* **18,** 113–124 (2014).

38. Kim, T.-H. *et al.* The Current Move of Lithium Ion Batteries Towards the Next Phase. *Adv. Energy Mater.* **2,** 860–872 (2012).

39. Shao, M., Ma, D. D. D. & Lee, S.-T. Silicon Nanowires - Synthesis, Properties, and Applications. *Eur. J. Inorg. Chem.* **2010,** 4264–4278 (2010).

40. Ellis, B. L., Lee, K. T. & Nazar, L. F. Positive Electrode Materials for Li-Ion and Li-Batteries †. *Chem. Mater.* **22,** 691–714 (2010).

41. Larcher, D. & Tarascon, J.-M. Toward greener and more sustainable batteries for electrical energy storage. *Nat. Chem.* 19–29 (2014).

42. Bauer, A. *et al.* Pt nanoparticles deposited on TiO2 based nanofibers: Electrochemical stability and oxygen reduction activity. *J. Power Sources* **195,** 3105–3110 (2010).

43. Zhang, X., Ji, L., Toprakci, O., Liang, Y. & Alcoutlabi, M. Electrospun Nanofiber-Based Anodes, Cathodes, and Separators for Advanced Lithium-Ion Batteries. *Polym. Rev.* **51,** 239–264 (2011).

44. Kushnir, D. & Sandén, B. a. Multi-level energy analysis of emerging technologies: A case study in new materials for lithium ion batteries. *J. Clean. Prod.* **19,** 1405–1416 (2011).

45. Li, J., Cao, C., Xu, X., Zhu, Y. & Yao, R. LiNi1/3Co1/3Mn1/3O2 hollow nano-micro hierarchical microspheres with enhanced performances as cathodes for lithium-ion batteries. *J. Mater. Chem. A* **1,** 11848 (2013).

46. Wu, Y., Cao, C., Zhu, Y., Li, J. & Wang, L. Cube-shaped hierarchical LiNi $_{1/3}$ Co $_{1/3}$ Mn $_{1/3}$ O $_2$ with enhanced growth of nanocrystal planes as high-performance cathode materials for lithium-ion batteries. *J. Mater. Chem. A* **3,** 15523–15528 (2015).

47. Patil, P. S. Versatility of chemical spray pyrolysis technique. *Mater. Chem. Phys.* **59,** 185–198 (1999).

48. Rao, V., Friedrich, K. A. & Stimming, U. *Handbook of Membrane SeparationsHandbook of Membrane Separations: Chemical, Pharmaceutical, Food, and Biotechnological Applications*. (CRC Press, 2009). doi:10.1111/j.1365-2621.2009.01974.x

49. Schaberg, M. S. *et al.* New Multi Acid Side-Chain Ionomers for Proton Exchange Membrane Fuel Cells. in *ECS Transactions* **33,** 627–633 (2010).

50. Zhang, H. & Shen, P. K. Recent development of polymer electrolyte membranes for fuel cells. *Chem. Rev.* **112,** 2780–832 (2012).

51. Rayne, S. & Forest, K. Perfluoroalkyl sulfonic and carboxylic acids: a critical review of physicochemical properties, levels and patterns in waters and wastewaters, and treatment methods. *J. Environ. Sci. Health. A. Tox. Hazard. Subst. Environ. Eng.* **44,** 1145–1199 (2009).

52. Wang, Z., Cousins, I. T., Scheringer, M. & Hungerbühler, K. Fluorinated alternatives to long-chain perfluoroalkyl carboxylic acids (PFCAs), perfluoroalkane sulfonic acids (PFSAs) and their potential precursors. *Environ. Int.* **60,** 242–248 (2013).

53. Wu, J. *et al.* A review of PEM fuel cell durability: Degradation mechanisms and mitigation strategies. *J. Power Sources* **184,** 104–119 (2008).

54. ReCiPe. ReCiPe Mid/Endpoint method, version 1.11. (2015).

55. Fiori, C. *et al.* Critical review of fuel cell's membranes and identification of alternative types for automotive applications. *Int. J. Hydrogen Energy* **40,** 11949–11959 (2015).

56. Chandan, A. *et al.* High temperature (HT) polymer electrolyte membrane fuel cells (PEMFC) – A review. *J. Power Sources* **231,** 264–278 (2013).

57. Wycisk, R., Pintauro, P. N. & Park, J. W. New developments in proton conducting membranes for fuel cells. *Curr. Opin. Chem. Eng.* **4,** 71–78 (2014).

58. Díaz, M., Ortiz, A. & Ortiz, I. Progress in the use of ionic liquids as electrolyte membranes in fuel cells. *J. Memb. Sci.* **469,** 379–396 (2014).

59. Scofield, M. E., Liu, H. & Wong, S. S. A concise guide to sustainable PEMFCs: recent advances in improving both oxygen reduction catalysts and proton exchange membranes. *Chem. Soc. Rev.* **44,** 5836–60 (2015).

60. He, G. *et al.* Nanostructured Ion-Exchange Membranes for Fuel Cells: Recent Advances and Perspectives. *Adv. Mater.* **27,** 5280–5295 (2015).

61. Subianto, S. Recent advances in polybenzimidazole/phosphoric acid membranes for high-temperature fuel cells. *Polym. Int.* **63,** 1134–1144 (2014).